# 國立交通大學

## 光電工程學系
## 顯示科技研究所

## 碩士論文

# 具角度調變之背光系統研究

# Study of Backlighting System with Angular Modulation

研究生 ：鍾積賢

指導教授：田仲豪 副教授

中 華 民 國 九 十 八 年 七 月

# 具角度調變之背光系統研究

# Study of Backlighting System with Angular Modulation


研 究 生：鍾積賢　　Student：Chi-Hsien Chang

指導教授：田仲豪　　Advisor：Chung-Hao Tien

國立交通大學 電機學院
光電工程學系
顯示科技研究所
碩士論文

**A Thesis**
**Submitted to Display Institute & Photonic Department**
**College of Electrical and Computer Engineering**
**National Chiao Tung University**
**in Partial Fulfillment of the Requirements**
**for the Degree of Master**
**in**
**Display Institute**
**July 2009**
**Hsinchu, Taiwan, Republic of China**

中華民國九十八年七月

# 具角度調變之背光系統研究

學生：鍾積賢　　指導教授：田仲豪 博士

國立交通大學
光電工程學系 顯示科技研究所

## 摘 要

本論文乃是根據超低耗能綠色顯示系統(Ultra-Low Power Eco LCD System)的概念，所提出一高效率低耗能的智慧型平面背光光源系統。其核心概念為利用發光二極體(Light Emitting Diode, LED)陣列與菲涅爾透鏡(Fresnel Lens)，組成一以菲涅爾透鏡之光軸為對稱軸且可調整出射光場角度之發光源系統。在本論文中，首先提出該光源系統實際之設置，藉由切換陣列中位於光軸或偏離光軸之 LED，提供正向模態(normal viewing mode)以及斜向模態(oblique viewing mode)等不同角度分佈的光場，並定義各模態之規範。除此之外，針對其角度分佈以及光場均勻性做進一步優化。利用此可調變光場角度的背光模組所組成之顯示器，可根據實際使用情況調變光源，在兼具經濟效益及節能考量之下，期望能達到一能依觀賞環境與觀賞者位置調整之智慧型多角度節能背光模組。

# Study of Backlighting System with Angular Modulation

**Student：Chi-Hsien Chang** **Advisor：Dr. Chung-Hao Tien**

**Department of Photonics & Display Institute**
**National Chiao Tung University**

## ABSTRACT

Aim at the concept of the Ultra-Low Power Eco LCD System, a smart planar backlighting system with high optical efficiency was proposed. The novel backlight system is composed of a light emitting diode (LED) array and cylindrical Fresnel lens. This lens can exhibit flexibility on angular distribution of the emitting optical field. In this thesis, the opto-mechanism setup and the niches of a backlight system would be introduced, discussed how to provide the normal and oblique viewing modes via controlling the LEDs individually. Furthermore, issues of the backlight system on angular distribution and uniformity would be optimized. In addition, the display subject to the above backlight module could reduce the power consumption and improve the economic efficiency by adjusting the LED power ratio. According to the observer's direction, a viewing switchable backlight can be modulated with different angular distribution.

# 致謝

首先要感謝我的指導教授田仲豪老師，這幾年來在研究上、表達能力及生活細節上無私的細心指導，並且提供我們良好的研究環境，使我在碩士生涯對於光學原理與背光系統有深入的了解，並順利完成本論文。

在實驗室的日子裡，謝謝博士班學長姐們在學業及生活上的諸多關懷與照顧，除了在研究過程中提供許多寶貴的建議，也給予我在生活上許許多多的幫助，同時還要感謝同學們以及學弟妹們，謝謝你們的陪伴，讓我擁有數不盡的快樂回憶。

我要感謝我的家人，謝謝你們多年來的支持與鼓勵，給予我無止境的溫暖的關懷，讓我能夠無後顧之憂的研究與學習，並順利完成碩士學業。

謝謝所有陪伴過我並關心我的人，這份喜悅的心情，獻給你們。

# Table of Contents

**Abstract (Chinese) ……..i**

**Abstract (English) ……..ii**

**Acknowledgement ……..iii**

**Table of Contents ……..iv**

**Figure Captions ……v**

**Chapter 1 *Introduction* .....1**

1.1 Background .....1

1.1.1 Temporal Modulation : Field Sequential Color LCD……2

1.1.2 Spatial Modulation : High Dynamic Range LCD…….3

1.2 Motivation and Objective .....4

1.3 Organization of this thesis.....7

**Chapter 2 *Principle* .....8**

2.1 Reflection and Refraction .....8

2.2 Photometry and Radiometry .....10

2.3 Fresnel Lenses.....14

**Chapter 3 *Design and Simulations*.....17**

3.1 Introduction.....17

3.2 Proposed Module for Viewing-Angle-Switchable Backlight .....20

3.3 Simulation Results for VAS backlight Arrays.....31

**Chapter 4 *Experimental Results*.....33**

4.1 Instruction .....33

4.2 Light Source Properties.....33

4.3 Light Control Prism Layer : Fresnel Lens .....34

4.4 Experimental Setup.....36

4.5 Measurement Results : Normal and Oblique Viewing Modes……...37

**Chapter 5 *Conclusion and Future work* .....40**

5.1 Conclusion .....40

5.2 Future Work .....41

***Reference*** **.....43**

# Figure Captions

***Fig. 1.1*** *The display mechanism of FSC LCD.* ……..……2

***Fig. 1.2*** *Real world dynamic range with 14 orders of luminance magnitude* …...……3

***Fig.1.3*** *The HDR LCD can be regarded as the superposition of low resolution backlight and high resolution LC panel.* …….……4

***Fig.1.4*** *By sampling the original image I, the processed signal IL will be the input signal of the LED BLM forming a non-uniform field distribution.* …...…..…4

***Fig.1.5*** *The picture shows configuration of viewing angle switchable vertical alignment display. The viewing angular ranges of this LC panel can be controlled from a wide viewing ranges over 170° to a narrow viewing angle ranges approximately 60° in the horizontal direction.*.....6

***Fig.1.6*** *The dual light source backlight system provides a function of adjustable viewing angles via electrically switching on either or both of dual light guide plates. According to different application purposes, the user can choose different viewing angular ranges.* …...……..……..…6

***Fig. 1.7*** *Schematic diagram of novel backlight system and the viewing direction of the viewer* ……..……..……...…….……..…7

***Fig. 2.1*** *(a) Reflection (b) Refraction.* ……..……..…8

***Fig. 2.2*** *A ray propagates through a prism.* …….……..…..…10

***Fig. 2.3*** *Schematic presentation for solid angle.* ….....…12

***Fig. 2.4*** *Simple radiometry problem : illuminance of a point source.* …….…...…12

***Fig. 2.5*** *The unit of radiometric and photometric.* ……..…13

***Fig. 2.6*** *The schematic structure form conventional continuous surface to Fresnel lens.* ……...…14

***Fig. 2.7*** *Grooves out type of Fresnel lens.* …….…...…..…15

***Fig. 2.8*** *Grooves in type of Fresnel lens.* ……...…...……..…16

***Fig. 3.1*** *(a) Brightness map and (b) angular distribution of common BL.* ……..…17

***Fig. 3.2*** *The 9 points method for uniformity measurement.* …….…….…18

***Fig. 3.3*** *Schematic presentation for desired viewing angle switchable display*…..…..19

***Fig. 3.4*** *Schematic presentation for desired angular distribution*……..….19

***Fig. 3.5*** *(a) On-axis source provide collimating rays in normal direction. (b) Oblique*

*direction rays via off-axis light source.……...….21*
***Fig. 3.6*** *Schematic configuration of proposed backlight module. ……..…22*
***Fig. 3.7*** *The actual setup of proposed backlight module in 3-D. …….……22*
***Fig. 3.8*** *The angular distribution of normal viewing mode with various distances in radar sketch. ……..…23*
***Fig 3.9*** *The FWHM of angular distribution V.S. various distances in normal viewing mode. ……..…23*
***Fig. 3.10*** *The simulation results of radar sketch with various distances in oblique mode. The higher distance had inadequate angle for oblique viewing mode and the FWHM of the angular distribution was too wide to use in lower distance. ……...……...……..…24*
***Fig. 3.11*** *The FWHM V.S. various distances at oblique viewing mode. The lower distances caused the inadequate FWHM. ……..…….…..…25*
***Fig. 3.12*** *The illuminance map of normal viewing mode. There was a hot zone at the center in this map and the uniformity was lower than 70%. ……...…25*
***Fig. 3.13*** *1-D linear light source and illumination distribution. ……...…26*
***Fig. 3.14*** *The blue line represented illuminance distribution via point source and the designed luminance intensity was red curve. ……..…..…27*
***Fig. 3.15*** *The gray line represented the simulation curve which could fit the* $cos^2\theta$ *approximation. ……..…..……..…28*
***Fig. 3.16*** *The light sources could be separated into three directions based on theoretic result to make the inverse cosine-square distribution, and then the hot spot issue could be fixed. ……..…28*
***Fig.3.17*** *The new opto-mechanical structure of VAS backlight unit and the middle section (CDE) was used for normal viewing mode, and the other cluster (AB, and GF) were used for oblique viewing mode. ……...……..…29*
***Fig. 3.18*** *A 7 inch prototype was constructed by three sections of LED backlight units with the Fresnel lens. ……29*
***Fig. 3.19*** *The simulation outcomes of normal mode uniformity and the red line was in horizontal direction. ……..…30*
***Fig. 3.20*** *The simulation outcomes of angular distribution in normal mode. ……30*
***Fig. 3.21*** *The simulation setups for (a) normal viewing mode and (b) oblique viewing mode in the optical simulation tool. ……..…31*
***Fig. 3.22*** *The simulation result of uniformity in normal viewing mode. …….…...…31*
***Fig. 3.23*** *The angular distribution of normal viewing modeand the FWHM was +/-20°. ……...……..…..…32*
***Fig. 3.24*** *The (a) uniformity and (b) angular distribution of oblique mode. ……..…32*
***Fig. 4.1*** *The white light LED light bar (iLED L03). …….……..…33*

***Fig. 4.2*** *Spectrum distribution of white light LED light bar (iLED L03).* ……..…*34*
***Fig. 4.3*** *The Edmund cylindrical Fresnel lens* ……*35*
***Fig.4.4*** *The Schematic configuration of entire mechanism setup for the actual VAS backlight module* ……..…*36*
***Fig. 4.5*** *The combined Fresnel lens* ……*36*
***Fig. 4.6*** *The apparatus was demonstrated which included the upper Fresnel lens and the bottom LED light bars.* ……..…..…*37*
***Fig.4.7*** *The entire VAS backlight module that we've manufactured was turned on.* ……..……..……..……..…*37*
***Fig.4.8*** *(a)The luminance map and the cross-sectional luminance curve with the uniformity of normal viewing modes was 80%; (b) The angular distribution of normal viewing mode with the FWHM +/- 20° by integral sphere.* ……..……..…*38*
***Fig.4.9*** *(a)The luminance map and the cross-sectional luminance curve with the uniformity of oblique viewing modes was 75%; (b) The angular distribution of oblique viewing mode with the FWHM +/- 20° by integral sphere..* ……*39*
***Fig. 5.1*** *Total performances of our VAS backlight in normal and oblique mode for normal and oblique viewing.* ……..……..…*41*
***Fig. 5.2*** *The Fresnel lens shall be replaced by a designed prism layer to improve the ability of light ray (i.e. green line) redirection for each mode.* ……..…*42*
***Fig. 5.3*** *The designed package for LED light bar can meliorate the uniformity and stray light issue of the VAS backlight.* ……..…..…*42*

# Table Captions

***Table 2.1*** *Factors for calculating reflection and refraction at the prism.* ……..…*10*
***Table 2.2*** *Radiometry Quantities* ……..……..……*11*
***Table 2.3*** *Photometry Quantities* ……..……..……*13*
***Table 3.1*** *Design target of VAS backlight system.*.....*20*
***Table. 4.1*** *Electrical and optical characteristics of LED light bar.* ……..……..…..…*35*
***Table. 4.2*** *The specifications of Edmund Fresnel lens.* ……..……..…*35*
***Table. 5.1*** *The comparison between direct and tunable type backlight module.* ……*41*

# Chapter 1

# Introduction

## 1.1 Background

Because the TV-affiliated activity occupies 10% of whole household power usage, developing a power saving ecologically friend display (Eco-display) become an important issue. In viewpoint of liquid crystal display (LCD), the requirements of conventional backlight module (BLM) including high steadiness, high brightness and uniformity is not satisfied for market expectations. The BLM with high efficiency and low power consumption which fabricated by environmental friendly materials has high potential for application to flat panel displays (FPDs) in near future.

According to the restriction of hazardous substances directive (RoHS) by European Union (EU), the cold cathode fluorescent lamps (CCFLs) in BLM will be replaced by mercury free LED as the light source in the oncoming market. Furthermore, LED has many advantages, such as small form factor, mercury free, long lifetime, fast switching operation, high power efficiency, and wide color gamut. In addition, the radiation efficiency of CCFLs about 60~90 lm/w is surmounted by white light LED which radiation efficiency is 136 lm/w [1]. With the high colorfulness and optical efficiency, LED is much suitable to be a next-generation LCD light source.

For the purpose of power saving, BLM will be the major component of Eco-Display. The LED BLM provides not only high brightness and uniformity, but also provides the temporal and spatial light modulation for LC panel. Therefore, the principles of these two modulation methods in LED backlight system will be introduced later.

### 1.1.1 Temporal Modulation : Field Sequential Color LCD [2-4]

In conventional LCD, color images are displayed by utilizing three individual color filters (CFs) which selectively present the Red, Green, and Blue (R, G, and B). However, only 33% light emitted from backlight could pass through the CFs, while the other 66% energy is absorbed. Therefore, the CF free display is one of the solutions to improve the optical efficiency in LCD. Recently, Field-Sequential-Color technology was proposed to provide a CF free solution. The FSC LCD included a fast-response LC panel and a LED backlight module which flashed with a R-G-B sequence to replace CFs in general LCD. Thus, human could watch the actual image by driving R, G, and B LEDs sequentially with corresponding LC signals in each frame time. As the Fig. 1.1 shows, the temporal mixing method divides full color images into R, G, and B fields in a frame. Compared with conventional LCD, FSC LCD has several advantages, such as high optical throughput, wide color gamut, low material cost and high screen resolution. In summary, such FSC BLM are different from the traditional BLM which was always in the full on state, and this method could also reduce the power consumption of BLM from 50% to 80%.

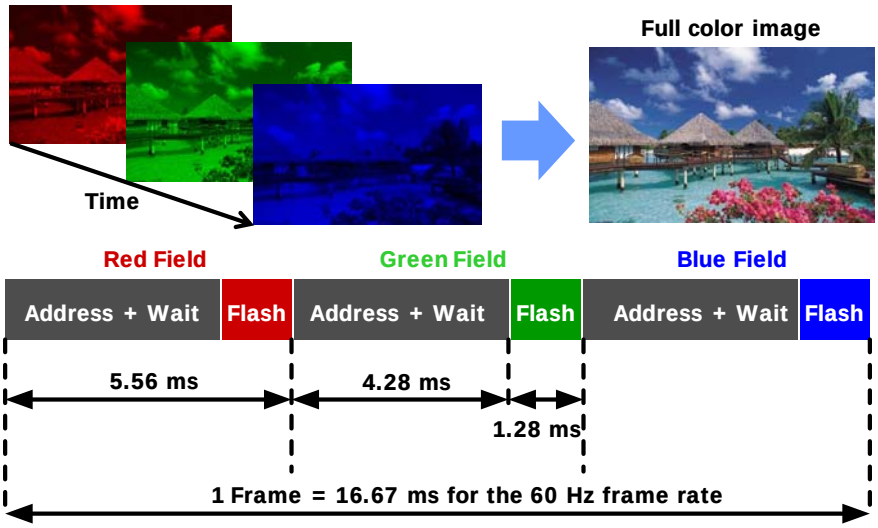


**Fig. 1.1** The display mechanism of FSC LCD

### 1.1.2 Spatial Modulation : High Dynamic Range LCD [5]

In the real world, the dynamic range of luminance magnitude from starlight to sun light has over 10 orders. But, the dynamic range of general LCD is limited in three orders, as Fig. 1.2 shows. This limitation is because of the low contrast ratio caused by light leakage of LC panel in dark state under a global dimming backlight source. Therefore, the high dynamic range (HDR) technology using local dimming backlight system can improve the LCD contrast ratio, and further reduce the power consumption.

The hardware setup of HDR LCD was proposed by BrightSide technologies (2003). As shown in Fig. 1.3, HDR LCD is composed of a low resolution high-power-LED array and a high resolution LC panel. The backlight system is constructed by a matrix of individually addressable LEDs. According to different image signals, backlight system can support a non-uniform field distribution by driving some parts of LEDs. The image quality of LCD will be improved by appending this kind of light source. Fig. 1.4 shows the algorithm of HDR system proposed by nctu. By means of down sampling the original image signal I, the intensity of the individual LED will be determined and form a local dimming distribution.

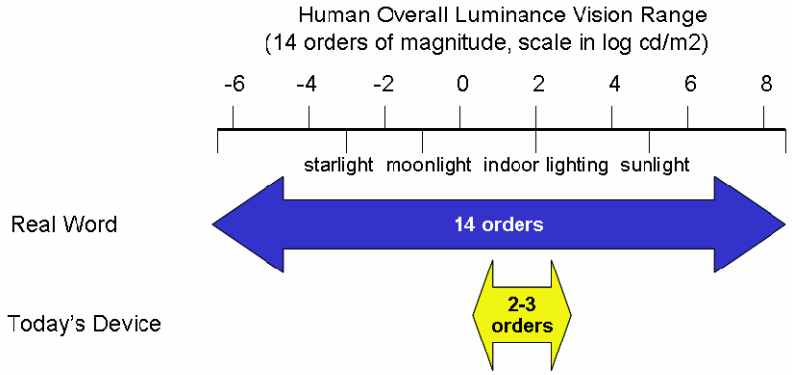


**Fig. 1.2** Real world dynamic range with 14 orders of luminance magnitude

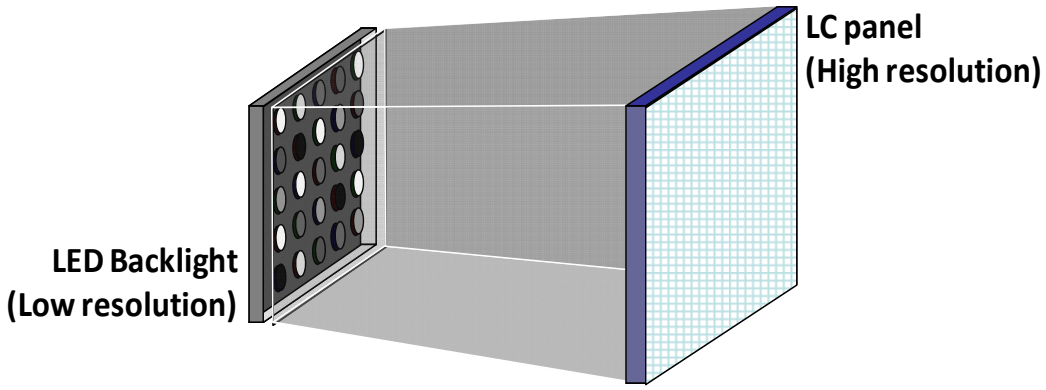


**Fig. 1.3** The HDR LCD can be regarded as the superposition of low resolution backlight and high resolution LC panel

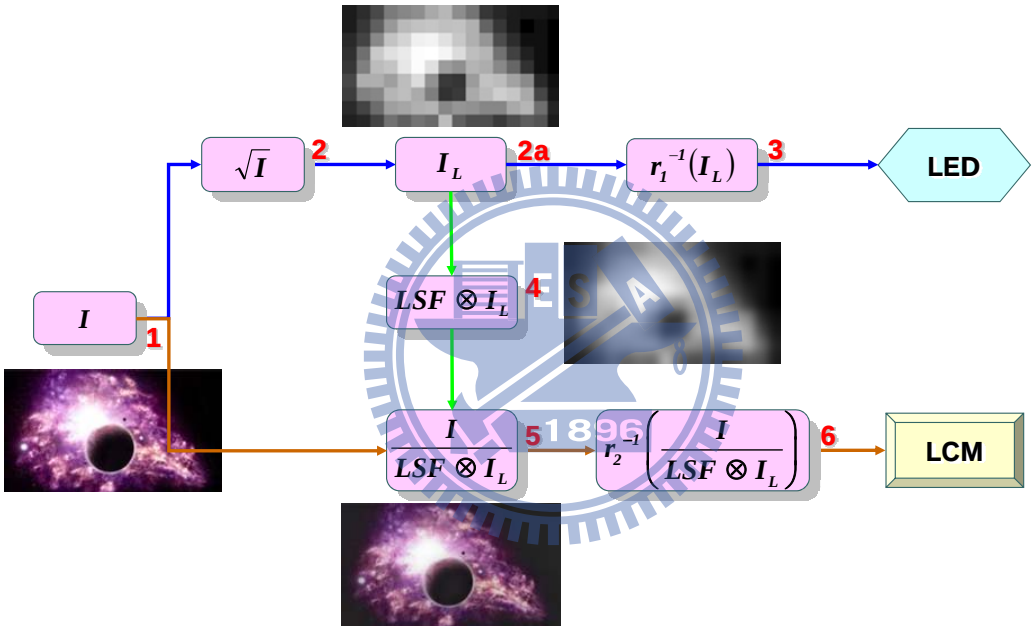


**Fig. 1.4** By sampling the original image I, the processed signal $I_L$ will be the input signal of the LED BLM forming a non-uniform field distribution.

## 1.2 Motivation and Objective

As the urgent request for multimedia applications, displays are supposed to be used for various purposes. For example, if a LCD is used as a television, a wide viewing angle shall be required to meet a lot of viewers' demand. In another case where the display is adopted for personal use in public places, it is desirable to reduce the viewing angle in order to keep the personal information confidential. In addition,

the viewing-angle switching technology is widely applied on 3-D display applications. Consequently, the viewing-adjustable LCD and its technical improvements is a topic that has been widely studied. Fig. 1.5 shows the configuration of viewing angle switchable LCD with additional VA layer [6]. The vertical alignment (VA) layer offers the wide viewing directions only if compensation films such as a negative C plate and a positive A plate are used. This compensation film, positive A plate, can be replaced by a homogeneous aligned (HA) liquid crystal layer, and the retardation of the HA layer at the off axis can be controlled by applying an electric field. Consequently, the viewing angular ranges of this LC panel can be controlled from a wide viewing ranges over 170° to a narrow viewing angle ranges approximately 60° in the horizontal direction. Some methods have been proposed for electrically controlling the viewing angles by the liquid crystal [7-9]. The main purposes are to reduce the contrast ratio as well as the light transmittance at the unnecessary directions [7]. However, the method might cause the low light efficiency and thicken the entire BL module which will hinder the practical use. Therefore, Fig 1.5 shows the dual light source backlight system to overcome these problems [10]. This dual light source backlight system provides a function of adjustable viewing angles via electrically switching on either or both of dual light guide plates. According to different application purposes, the user can choose different viewing angular ranges from 140° to 60° or less and luminous uniformity is over than 72%. Nonetheless, the configuration in Fig 1.6 limits the number of switching modes and causes light absorption in the additional light guide.

Instead of a complex design that places an additional light guide or a particular LC layer, the LED-based viewing-adjustable backlight unit is proposed in this study. The objective of the study is to design an optical setup with three directions as shown in Fig. 1.7. The normal mode (Zone I) and the oblique modes (Zone II, III) can be

individually turned on; therefore, a wide viewing field (dash line) is the combination of these three modes. The expected directions of oblique modes (oblique angle:α) should be switched by our design. If necessary, there are seven combinations at most for various situations. Furthermore, the design provides a potential way to practice the LCD with multi-viewing angles.

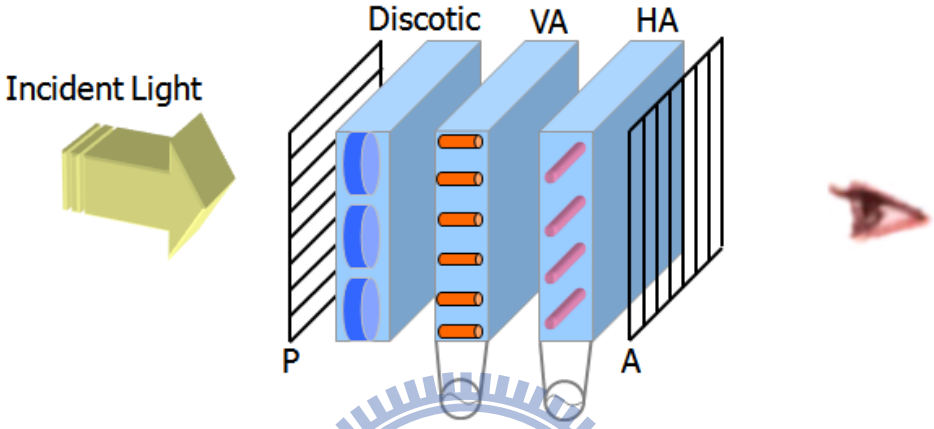


**Fig. 1.5** The picture shows configuration of viewing angle switchable vertical alignment display. The viewing angular ranges of this LC panel can be controlled from a wide viewing ranges over 170° to a narrow viewing angle ranges approximately 60° in the horizontal direction.

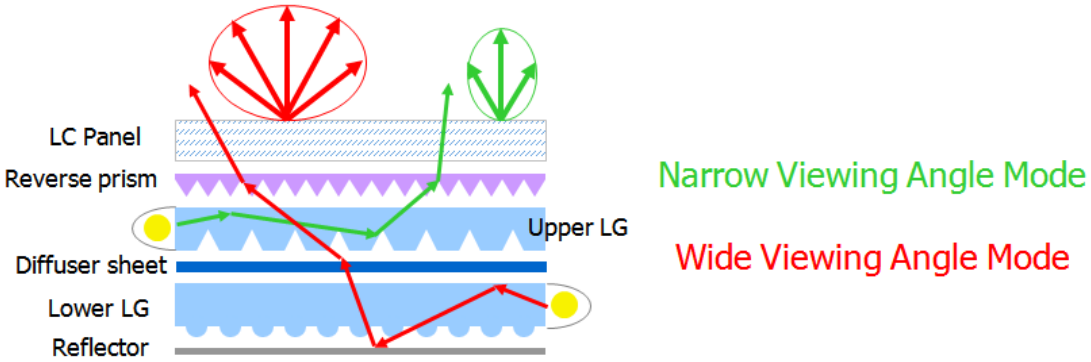


**Fig. 1.6** The dual light source backlight system provides a function of adjustable viewing angles via electrically switching on either or both of dual light guide plates. According to different application purposes, the user can choose different viewing angular ranges.

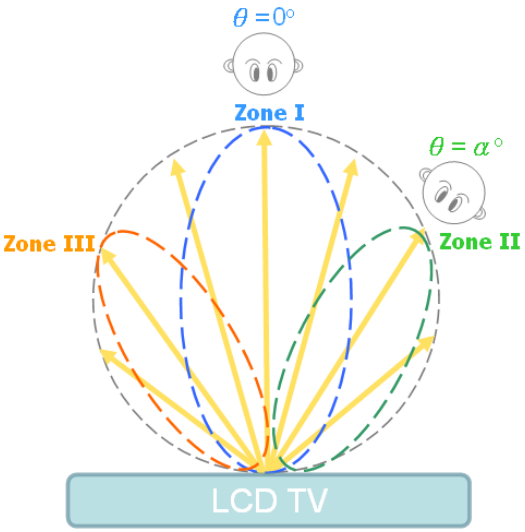


**Fig. 1.7** Schematic diagram of novel backlight system and the viewing direction of the viewer

## 1.3 Organization of this Thesis

This thesis is organized as follows. First, Chapter 2 will explain how the Fresnel lens system works, and the principles of radiometry and photometry will be described with more details. In Chapter 3, the opto-mechanism design and simulations of our module will be presented. The Chapter 4 is the experimental result and discussion. Finally, the summary of this thesis and future works will be presented in Chapter 5.

# Chapter 2

# Principle

## 2.1 Reflection and Refraction [11]

In geometrical optics, reflection and refraction are two basic principles. When the ray travels from one medium to another, it will be reflected and/or refracted. The schematic for reflection and refraction in two-dimensional case is shown in Fig. 2.1.

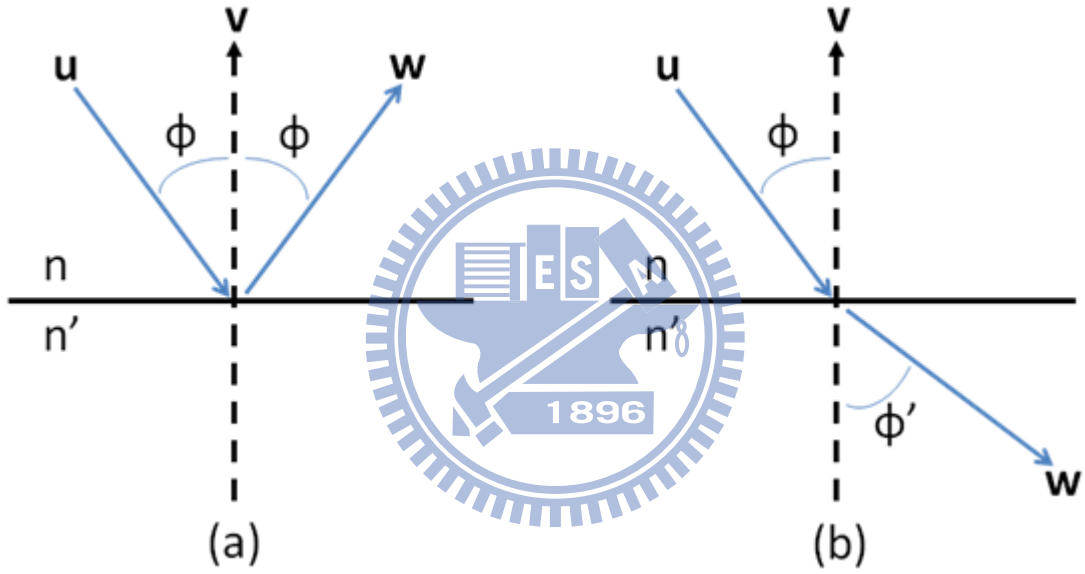


**Fig. 2.1** (a) Reflection (b) Refraction

In Fig. 2.1(a), it shows two mediums with different refractive indexes, n and n', and the incident ray **u** hits the interface. The dotted vector **v** is the normal vector of the boundary surface. And the vector **u** is reflected as the vector **w** at the boundary. The incident angle $\phi$ equals to the angle of reflection. Therefore, the reflection can be characterized by this factor.

By linear algebra, the vector **w** can be formed by vector **u** and **v**.

$$\mathbf{w} = a\mathbf{u} + b\mathbf{v} \tag{2.1}$$

The equation (2.1) can be rewritten by scalar multiplication by **u**

$$\mathbf{u}\cdot\mathbf{w} = a(\mathbf{u}\cdot\mathbf{u}) + b(\mathbf{u}\cdot\mathbf{v}) \tag{2.2}$$

When the vectors, **u**, **v**, and **w**, are unit vectors, the equation (2.2) can be expressed as

$$-\cos 2\phi = a - b\cos\phi \tag{2.3}$$

By the same process, scalar multiplication with **v** yields the similar expression

$$\mathbf{v}\cdot\mathbf{w} = a(\mathbf{v}\cdot\mathbf{u}) + b(\mathbf{v}\cdot\mathbf{v}) \tag{2.4}$$

$$\cos\phi = -a\cos\phi + b \tag{2.5}$$

Because of linearly independent, the Cramer's rule can be applied to solve the unknown coefficients in these equations. Finally, the coefficients a and b can be calculated to be

$$a = \frac{\begin{vmatrix} -\cos 2\phi & -\cos\phi \\ \cos\phi & 1 \end{vmatrix}}{\begin{vmatrix} 1 & -\cos\phi \\ -\cos\phi & 1 \end{vmatrix}} = \frac{\sin^2\phi}{\sin^2\phi} = 1 \tag{2.6}$$

$$b = \frac{\begin{vmatrix} 1 & -\cos 2\phi \\ -\cos\phi & \cos\phi \end{vmatrix}}{\begin{vmatrix} 1 & -\cos\phi \\ -\cos\phi & 1 \end{vmatrix}} = -2\cos\phi \tag{2.7}$$

Contrary to the reflection case, the incident angle $\phi$ do not equal to refractive angle $\phi'$ in Fig 2.1(b), but obey the Snell's law

$$n\sin\phi = n'\sin\phi' \tag{2.8}$$

However, the coefficients a and b can receive by the similar procedure. After applying the scalar multiplication in equations (2.2) and (2.4), the equations is given by

$$\cos(\phi - \phi') = a - b\cos\phi \tag{2.9}$$

$$-\cos\phi' = -a\cos\phi + b \tag{2.10}$$

Using the sum and difference formula of trigonometric function and the Cramer's rule, the coefficients a and b can be obtained,

$$a = \frac{\begin{vmatrix} \cos(\phi-\phi') & -\cos\phi \\ -\cos\phi' & 1 \end{vmatrix}}{\begin{vmatrix} 1 & -\cos\phi \\ -\cos\phi & 1 \end{vmatrix}} = \frac{\sin\phi'}{\sin\phi} = \frac{n}{n'} \tag{2.11}$$

$$b = \frac{\begin{vmatrix} 1 & \cos(\phi-\phi') \\ -\cos\phi & -\cos\phi' \end{vmatrix}}{\begin{vmatrix} 1 & -\cos\phi \\ -\cos\phi & 1 \end{vmatrix}} = -\cos\phi' + \frac{n}{n'}\cos\phi \qquad (2.12)$$

According to the results mentioned above, a ray entering a prism can be realized as three cases. And these outcomes have been represented in Fig 2.2 and tabulated in Table 2.1.

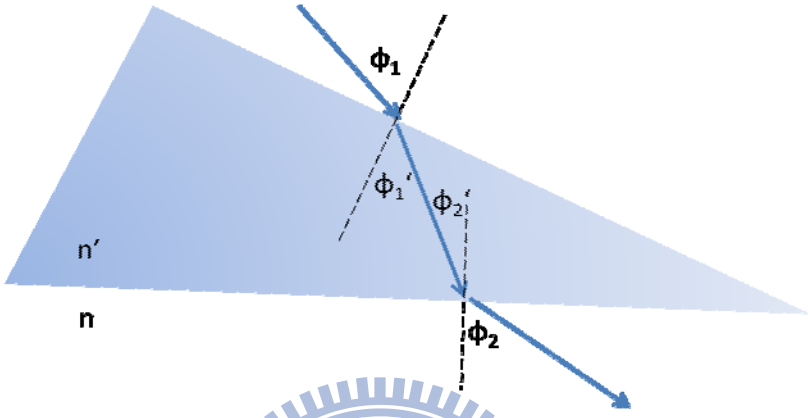


**Fig. 2.2** A ray propagates through a prism

**[Table 2.1]** Factors for calculating reflection and refraction at the prism

| | Factor a | Factor b |
|---|---|---|
| **Refraction at the prism's first surface** | n/n' | $-\cos\phi_1' + (\frac{n}{n'})\cos\phi_1$ |
| **Refraction at the prism's second surface** | n'/n | $-\cos\phi_2' + (\frac{n'}{n})\cos\phi_2$ |
| **Reflection at the prism's second surface** | 1 | $-2\cos\phi_2$ |

## 2.2 Photometry and Radiometry

Radiometry is a science which is used to measure the light in any portion of the electromagnetic spectrum. In any optical systems, the distribution of radiation energy

is a very important issue. Therefore, the radiation must be defined clearly. The fundamental radiometric quantities are shown in Table 2.2.

**[Table 2.2]** Radiometry Quantities

| Quantity | Symbol | Definition | Typical Units |
|---|---|---|---|
| **Radiant Energy** | Q | | Joule(J) |
| **Radiant Flux** | φ | dQ/dt | Watt(W) |
| **Radiant Intensity** | I | dφ/dw | Watt/sr |
| **Radiance** | L | dφ/cosθdAdw | Watt/sr·$m^2$ |
| **Irradiance** | E | dφ/dA | Watt/$m^2$ |
| **Radiant Exitance** | M | dφ/dA | Watt/$m^2$ |

The radiant energy Q indicates the propagating energy of electromagnetic radiation. In some applications, the radiation energy can be realized as the collection of photons, and the energy of a single photon is hυ.

The radiant flux φ is the the rate of flow of the energy with respect to time, dQ/dt, and the unit is Watt (W).

The radiant intensity I is power per unit solid angle. The angle which seen from the center of a sphere includes a given area on the surface of that sphere. [Fig. 2.3] The value of the solid angle is numerically equal to the size of that area divided by the square of the radius of the sphere.

Radiance is the flow of the power with respect to the solid angle and projected area, dφ/dωdAcosθ. And θ is the angle between the surface normal vector and the specified direction.

Irradiance is the power per unit area incident from all direction in a hemisphere whose base is that surface. The symbol is E. A similar quantity is radiant exitance, which is the power per unit area leaving a surface to a hemisphere whose base is that

surface. The symbol is M.

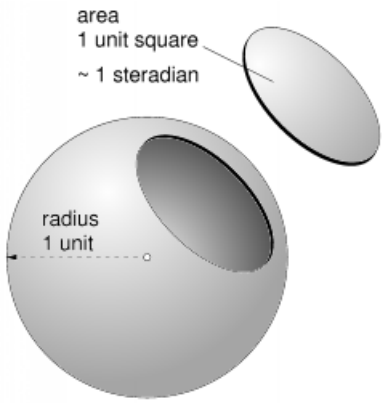


**Fig. 2.3** Schematic presentation for solid angle

For example, there is a small lambertian point source and the radiant intensity $I_s$ which is independent of direction. [Fig. 2.4] The irradiance $E_d$ of the detected area $dA_d$ on the illumination screen is derived from

$$d\Phi_d = I_s\left(\frac{dA_d\cos\theta}{r^2}\right) = I_s\frac{dA_d\cos\theta}{(z/\cos\theta)^2} = \frac{I_s dA_d\cos^3\theta}{z^2}$$

$$E_d = \frac{I_s\cos^3\theta}{z^2} \qquad (2.13)$$

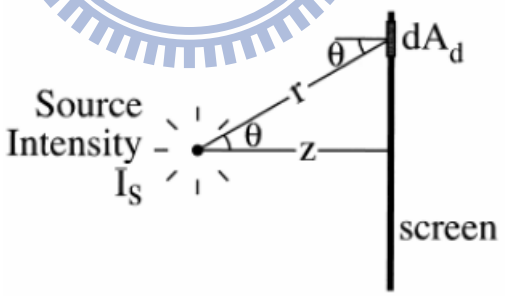


**Fig. 2.4** Simple radiometry problem : illuminance of a point source

As shown in [Fig. 2.4], where z is the normal distance from source to screen, and r is equal to z/cosθ . The equation (2.13) shows the $\cos^3\theta$ law, which is conventionally stated: For a small point source, the irradiance on a flat surface is direct proportional to cubic of cosθ.

Photometry is the measurement of light which is defined as electromagnetic

radiation that is detectable by the human eye. This range corresponding to wavelength is 380 to 830 nanometer (nm). Unit symbols are subscripted with v to denote visible, and unit names are prefixed with the term luminous. The unit of luminous flux ($\varphi_v$) is called a lumen (lm). The fundamental photometric quantities are similar to the radiometric as shown in Table 2.3. The difference between radiometry and photometry is that the radiometry includes the entire optical radiation spectrum, while photometry is limited to visible spectrum as defined by response of human eye. Fig.2.5 shows the both measurement system.

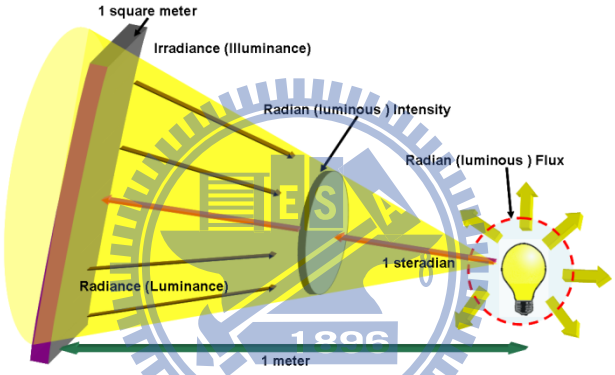


**Fig. 2.5** The unit of radiometric and photometric

**[Table 2.3]** Photometry Quantities

| Quantity | Symbol | Definition | Typical Units |
|---|---|---|---|
| **Luminous Energy** | $Q_v$ | | lm·s |
| **Luminous Flux** | $\varphi_v$ | $dQ_v/dt$ | lumen(lm) |
| **Luminous Intensity** | $I_v$ | $d\varphi_v/dw$ | lm/sr |
| **Luminous** | $L_v$ | $d\varphi_v/\cos\theta dAdw$ | $lm/sr{\cdot}m^2$ |
| **Illuminance** | $E_v$ | $d\varphi_v/dA$ | $lm/m^2$ |
| **Luminous Exitance** | $M_v$ | $d\varphi_v/dA$ | $lm/m^2$ |

## 2.3 **Fresnel lenses** [12]

A Fresnel lens is an optical component which can be used as a cost-effective, lightweight alternative to conventional continuous surface optics as shown in Fig. 2.5.

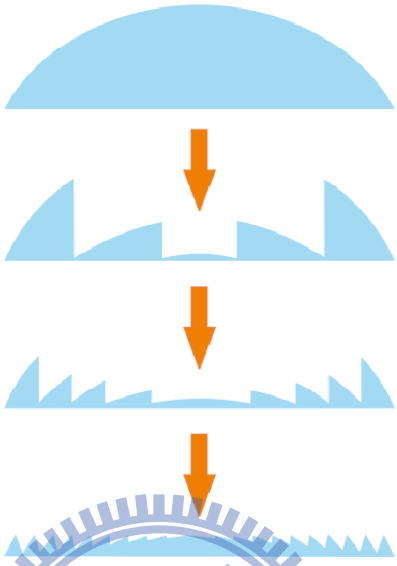

**Fig. 2.6** The schematic structure form conventional continuous surface to Fresnel lens

The design of some simple Fresnel lens will be presented in this section. A grooves-out design directs the facets towards the side of the collimated beam and a grooves-in design orients the facets towards the focal point. Then the Fresnel lens converts a point source to a beam of parallel light as a collimator.

**Grooves Out** [13]

By Fig 2.6, a set of four equations can be derived.

$$\sin\alpha = n\sin\beta \tag{2.14}$$

$$-\alpha = \gamma - \beta \tag{2.15}$$

$$n\sin\gamma = \sin\omega \tag{2.16}$$

$$\tan\omega = R/f \tag{2.17}$$

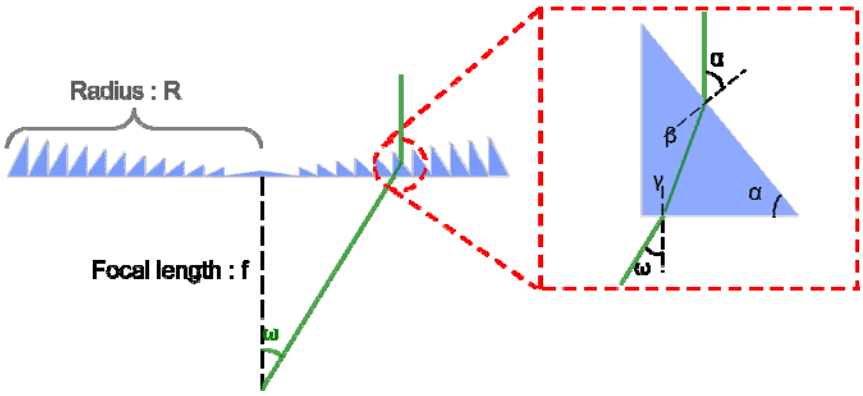


**Fig. 2.7** Grooves out type of Fresnel lens

An expression for $\tan\alpha$ can be obtained after some substitutions.

$$\tan\alpha = \frac{n\sin\gamma}{1-n\cos\gamma} \tag{2.18}$$

By multiplying and square root, the equation 2.16 can formed a new expression.

$$n\cos\gamma = \sqrt{n^2 - \sin^2\omega} \tag{2.19}$$

The final form from these equations is

$$\tan\alpha = \frac{\sin\omega}{1-\sqrt{n^2-\sin^2\omega}} \tag{2.20}$$

**Grooves In** [14]

In a very similar procedure, the Fresnel lens with grooves facing inwards will be presented. According to Fig. 2.7, three equations can be set up to describe this system.

$$n\sin\alpha = \sin\beta \tag{2.21}$$

$$\tan\omega = {}^{R}/_{f} \tag{2.22}$$

$$\beta = \alpha + \omega \tag{2.23}$$

Substituting $\beta$ in equation 2.21 with 2.23 yields an expression for $\tan\alpha$.

$$\tan\alpha = \frac{\sin\omega}{n-\cos\omega} \tag{2.24}$$

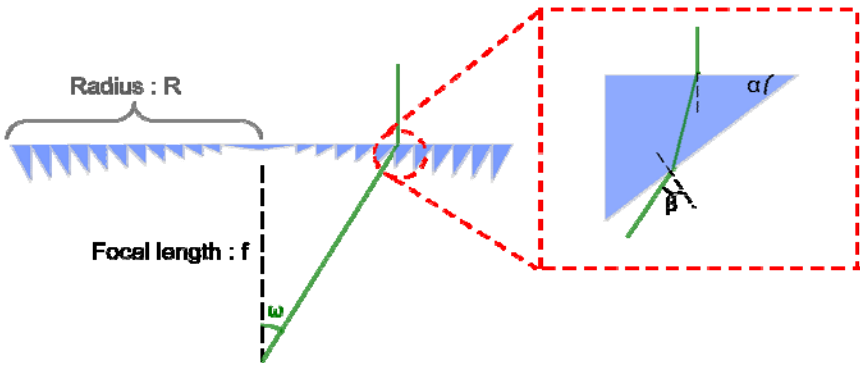


**Fig. 2.8** Grooves in type of Fresnel lens

Furthermore, equation 2.24 can express in terms of focal length f and aperture R.

$$\tan\alpha = \frac{R}{n\sqrt{R^2+f^2}-f} \tag{2.25}$$

# Chapter 3

# Design and Simulations

## 3.1 Introduction

In this chapter, all the design process and the simulation model of viewing-angle-switchable (VAS) backlight were established. Before entering the theme, the basic concept will be introduced briefly. Then the design targets will be decided. Subsequently, the light control film will be described in detail; meanwhile, the brief discussions and optimization processes for VAS backlight unit will be given. Therefore, the simulation model established to characterize the feature of the VAS backlight as well as the simulation results will also be presented. After all, the VAS backlight model was designed and optimized.

Firstly, the optical performances of the traditional backlight module (direct-type backlight) are shown in below. Figure 3.1(a) is the brightness map with 25 points which could evaluate the uniformity of the backlight system. According to the panel sizes, it could choose different point numbers. The uniformity of VAS backlight was determined with the luminance level of the 9 points as shown the definition in Equation (3.1) and Figure 3.2.

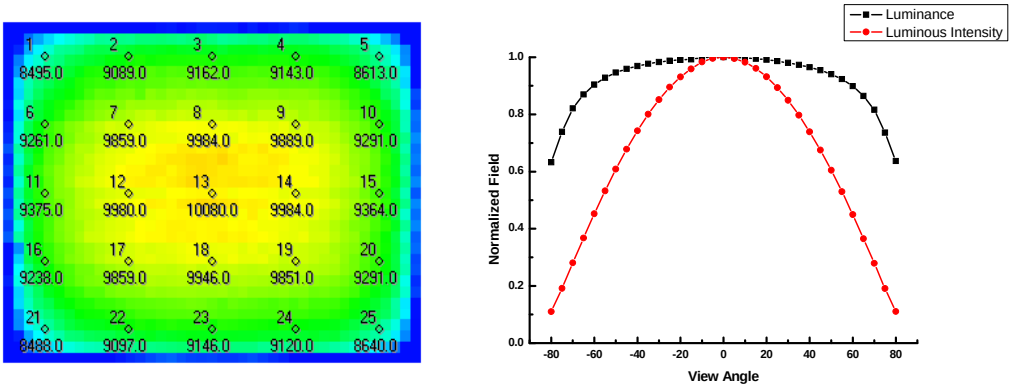


(a) (b)

**Fig. 3.1** (a) Brightness map and (b) angular distribution of common BL

$$\text{Uniformity} \equiv \frac{\text{Min}(P_1, P_2 \cdots P_n)}{\text{Max}(P_1, P_2 \cdots P_n)} \times 100\% \quad (3.1)$$

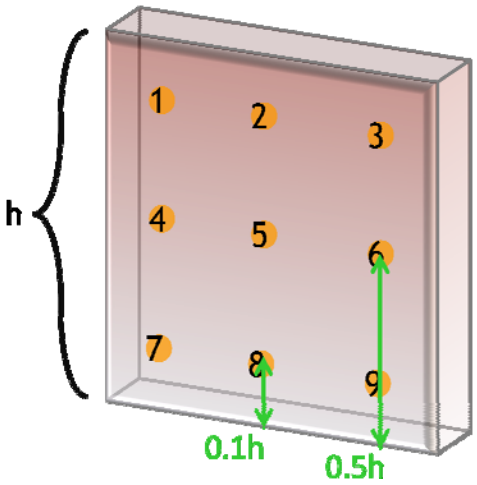


**Fig. 3.2** The 9 points method for uniformity measurement

Fig 3.1 (b) shows the angular distribution of traditional backlight module without brightness enhancement film (BEF). The black line in Fig. 3.1 (b) represents that the luminance is almost the same in any observing direction. Therefore, the traditional backlight could be seen as a lambertian light source with very high brightness and uniformity. After introducing the optical characteristics of traditional backlight, the concepts of VAS backlight will be discussed in the following.

In this thesis, we want to design a BLM which can offer the normal viewing mode as zone I and two oblique viewing modes as zone II and zone III as shown in Fig 3.3. The optical field distribution and the actual image are shown as these schematic presentations in Fig. 3.3. As these pictures, the left parts are the designed angular distribution with three different directions on backlight module and the right parts show the desired viewing situations in actual displays.

According to the schemes in the left parts of Fig. 3.3, the corresponding distribution on relative rectangular candela distribution is shown in Fig. 3.4. The desire angular distribution in Fig 3.4 used to compare with the simulation result of VAS backlight.

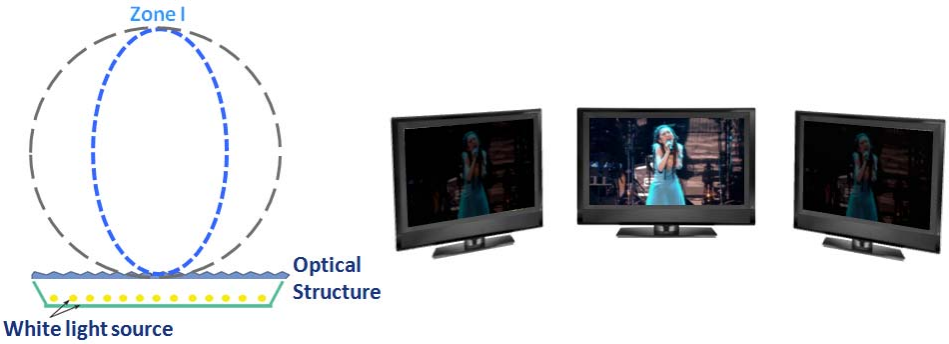


(a) Normal viewing mode

(b) Oblique viewing mode

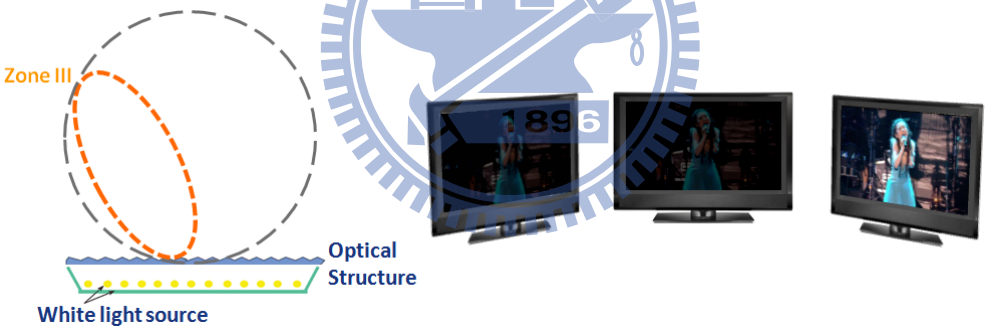


(c) Oblique viewing mode

**Fig. 3.3** Schematic presentation for desired viewing angle switchable display

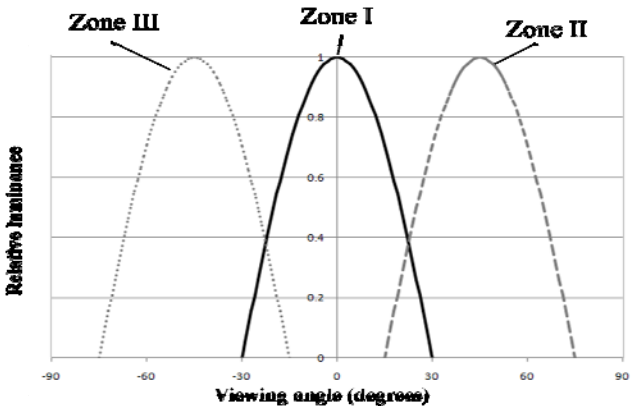


**Fig. 3.4** Schematic presentation for desired angular distribution

After the objective which mentioned in the introduction, the design targets were concerned here. Three main design parameters used to set the final goal for VAS backlight included luminance, FWHM of angular distribution, and the uniformity of entire backlight module, and these parameters were compared with common Notebook backlight requirement. Table 3.1 shows the design target of our VAS backlight. All of the requirements shown in this table are indicated that the luminance must be higher than 3500 nits, and the FWHM of viewing angle distribution confined in +/- 20 degrees, and the uniformity was higher than 70% for both normal and oblique viewing modes.

**[Table 3.1]** Design target of VAS backlight system

| Design Parameter | Luminance( nits ) | Viewing Angle ( FWHM ) | Uniformity ( 9pts. ) |
|---|---|---|---|
| NB BL Requirement | 3500~5000 | +/-40 deg | >70% |
| Normal Viewing | >3500 | +/-20 deg | >70% |
| Oblique Viewing | >3500 | +/-20 deg | >70% |

## 3.2 Proposed Module for Viewing-Angle-Switchable Backlight

As shown in Fig. 3.5, the divergent rays of point source can be refracted into collimating light by single lens (i.e., collimator) in geometrical optics. If the point light source located on the optical axis of lens as in Fig 3.5 (a), the output light would propagate along the direction of optical axis of this lens. When the point source located off the optical axis with the included angle α, the output rays would travel parallelly with the same angle as Fig 3.5 (b). From this simple idea, the viewing direction adjustable backlight system was possible by placing a lens in front of the light source and provides the directional optical field via different locations of the light sources. However, the lens shape would increase much thickness of entire

backlight module in practice. In order to overcome this problem, a designed light control film could used to replace the role of common lens to compose the VAS backlight.

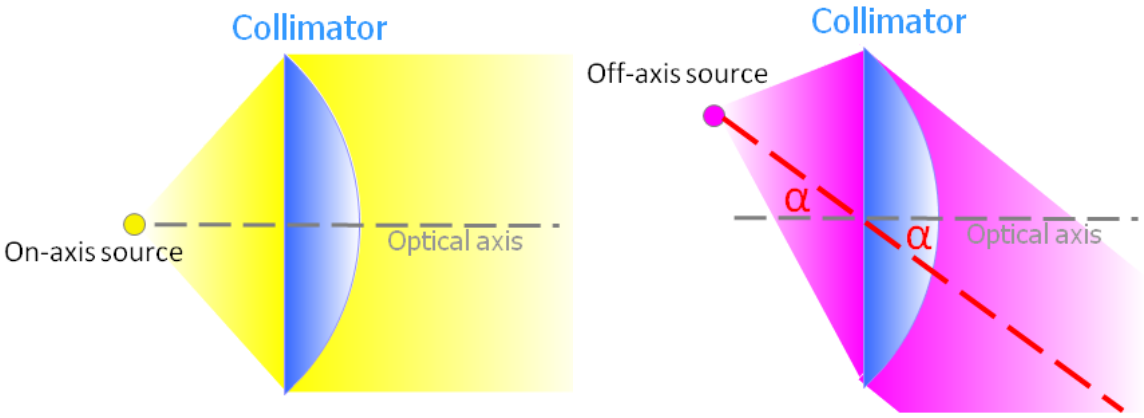


(a) (b)

**Fig. 3.5** (a) On-axis source provide collimating rays in normal direction.

(b) Oblique direction rays via off-axis light source.

After the basic concept of viewing angle control, the original opto-mechanism setup included the designed prism layer and three LED light bars as shown the cross-section in Fig 3.6, and Fig 3.7 is the scheme of three-dimensional picture. The normal mode is achieved by a designed prism layer and a LED light bar on the optical axis as the green rays in Fig. 3.6. In addition, the oblique mode is achieved by the same prism layer and an off axis LED light bar as the cyan rays. Because of the limit of size and the difficulty of manufacturing, a commercially available cylindrical Fresnel lens was used to replace the prism layer. In the following sections, the cylindrical Fresnel lens was called “Fresnel lens” in this thesis for convenience. The Fresnel lens played well a role in controlling the rays to provide directional optical fields and the peak value of the oblique direction is about 40 degrees.

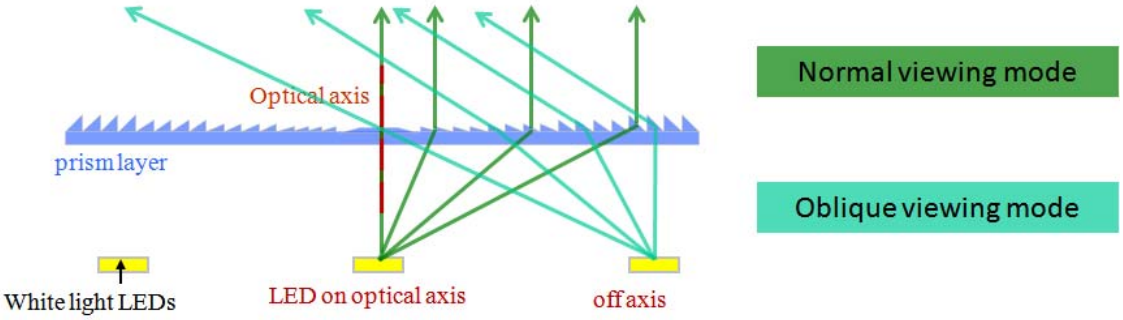


**Fig. 3.6** Schematic configuration of proposed backlight module

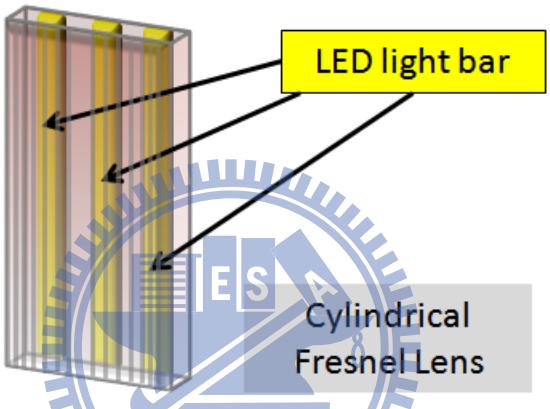


**Fig. 3.7** The actual setup of proposed backlight module in 3-D

In this opto-mechanism, two parameters could be adjusted: the distance from the surface of LED light bar to the Fresnel lens and the power radio of these LED light bars. Besides, the detail specification of Fresnel lens and LED light were added in chapter four. In addition, it deserved to be mentioned that the focal length of the Fresnel lens was 5 cm.

The distance (i.e. d) of parameter which mentioned above was the first concern in this design procedure. In the beginning, the main assignment was to find out the suitable distance of normal viewing mode. By this reason, we could simulate this configuration with difference operating distance by optical software (i.e. LightTools). The simulation results are shown as radar sketch in Fig. 3.8. According to Fig. 3.8, if

the LED light bar is held 5 cm (i.e. d = focal length) away from the Fresnel lens as the blue line, the angular distribution would be too sharp to apply on normal viewing mode. However, if the LED light bar is placed on the one-third of the focal length (i.e. d/3 = 1.67 cm) as the green line, the FWHM of the angular distribution would be too wide to use as the normal mode.

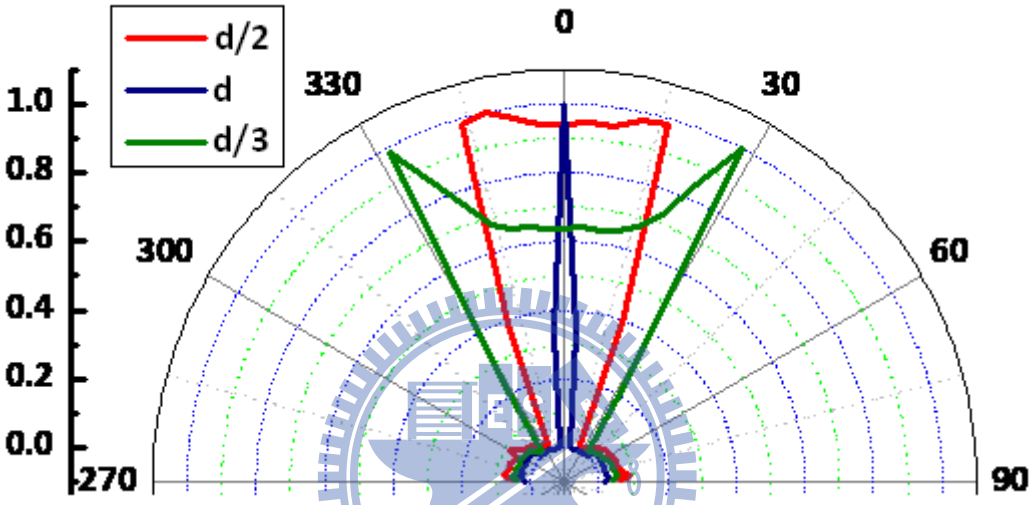


**Fig. 3.8** The angular distribution of normal viewing mode with various distances in radar sketch

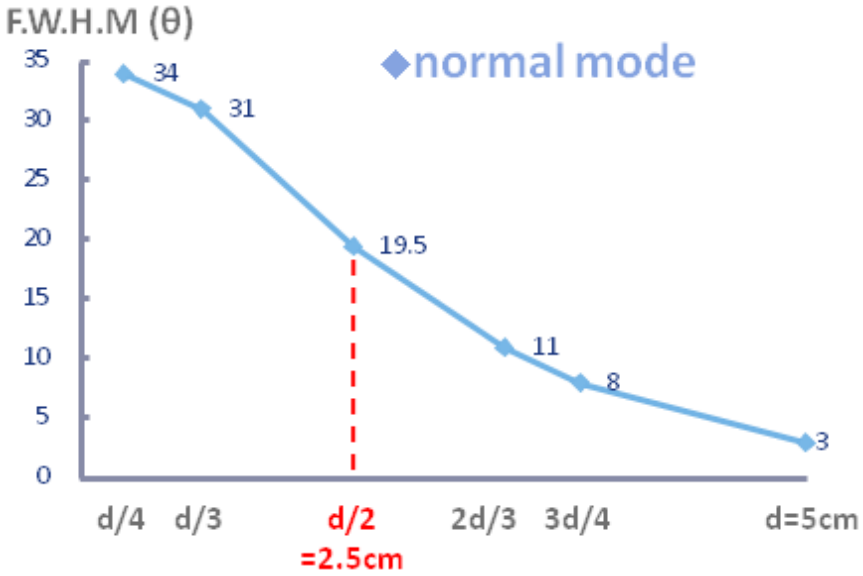


**Fig. 3.9** The FWHM of angular distribution V.S. various distances in normal viewing mode

Fig. 3.9 shows the relationship between FWHM and the distance d. According to the design parameters in Table 3.1, d/2 was the most suitable distance for our design target.

However, how about the optical performances of oblique viewing mode?

We could repeat the similar process by optical software to find out the angular distributions in oblique viewing mode. However, it did not easily make a decision like normal mode, and I would discuss in the following.

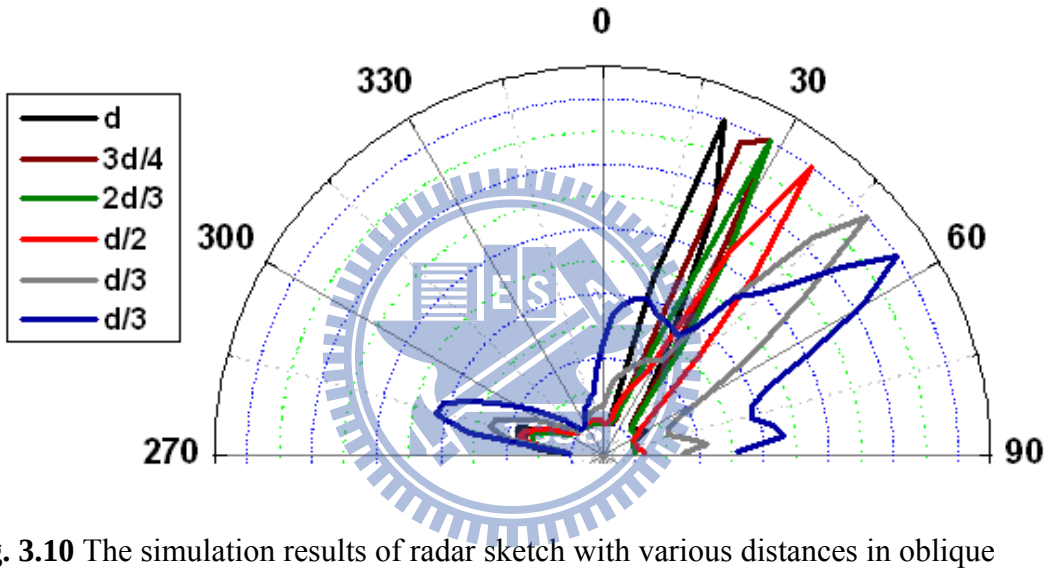


**Fig. 3.10** The simulation results of radar sketch with various distances in oblique mode. The higher distance had inadequate angle for oblique viewing mode and the FWHM of the angular distribution was too wide to use in lower distance.

According to Fig. 3.10 and Fig. 3.11, the higher distance have inadequate angle for oblique viewing mode and the FWHM of the angular distribution are too narrow to use as the black, brown, and the green lines. However, if the distance decreases to one-third focal length (i.e. d/3 = 1.67 cm), it will increase the FWHM for normal mode which shown in Fig. 3.8 and had much stray light in other viewing directions. Therefore, we have a trade-off between the normal and oblique modes. So, we chose

d/2 (i.e. half focal length 2.5 cm) as the distance between the Fresnel lens and LED light bars. After the distance chosen by the simulation results above, the simulation of our opto-mechanism could be started. And the simulation result was shown in Fig. 3.12.

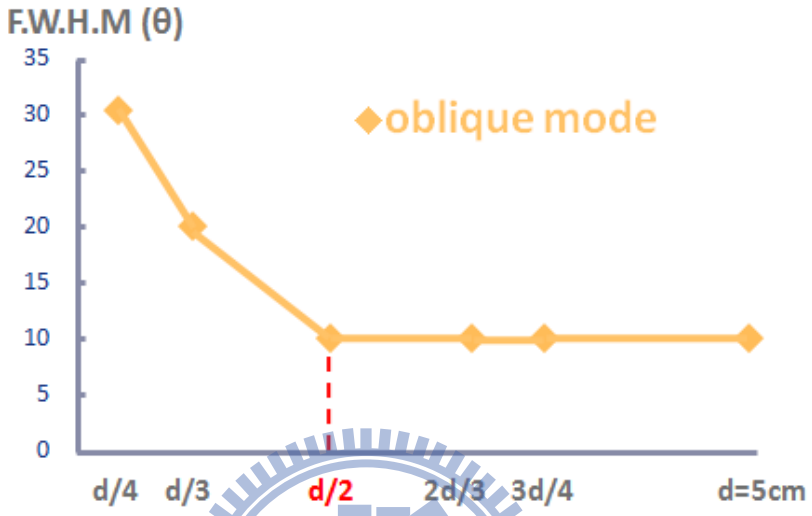


**Fig. 3.11** The FWHM V.S. various distances at oblique viewing mode. The lower distances caused the inadequate FWHM.

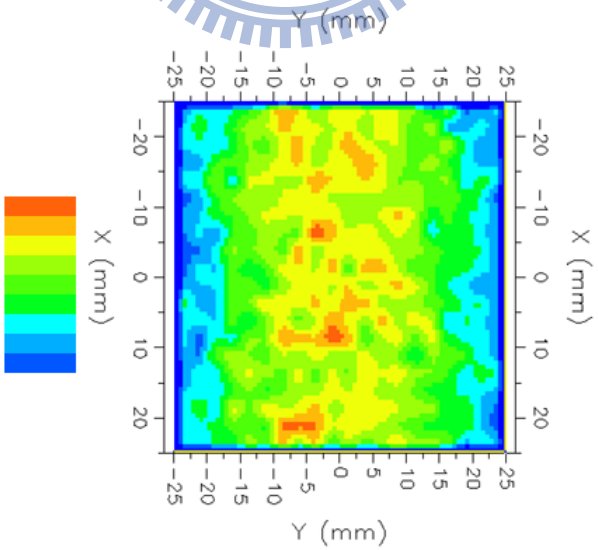


**Fig. 3.12** The illuminance map of normal viewing mode. There was a hot zone at the center in this map and the uniformity was lower than 70%.

By Fig. 3.12, there was a hot spot area appear by using this simple setup as the VAS backlight, and the poor uniformity of normal and oblique mode was the chief defect in this configuration.

In order to solve the uniformity problem, we could review the photometry example shown in Fig 2.4. The result was equation (2.13) which also means the $\cos^3\theta$ law. It meant that the irradiance on a flat surface which illuminated by a small point source was direct proportional to cubic of $\cos\theta$. Therefore, the main purpose of this study was to modify the viewing angle of observer in a horizontal direction in VAS backlight. Via this way, we could reduce the dimension of screen in Fig 2.4 from 3-D into 1-D. Similar to the process mentioned in chapter 2, the deriving details were shown below.

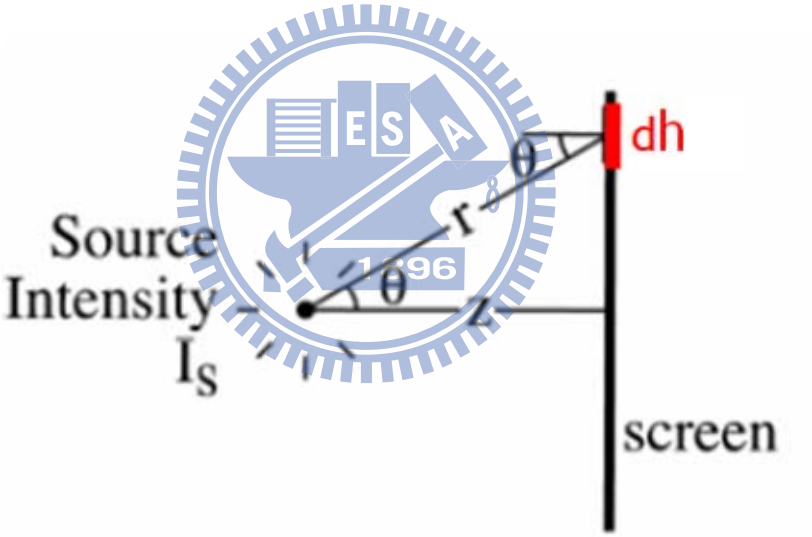


**Fig. 3.13** 1-D linear light source and illumination distribution

$$I = \frac{d\Phi}{d\theta}$$

$$dh = rd\theta$$

$$d\Phi_d = I_s \frac{dh\cos\theta}{r}$$

$$= I_s \frac{dh\cos^2\theta}{z}$$

$$E_{screen} = I_s \frac{\cos^2\theta}{z} \quad (3.2)$$

According to equation (3.2), the illumination distribution of a point source was proportional to $\cos^2\theta$, and the hot spot issue was formed by this term. Therefore, we could use this property to increase the uniformity of the VAS backlight. As shown in Fig 3.8, the blue line represents the illumination curve caused by the point source. If the source intensity, $I_s$, proportioned to $\cos^{-2}\theta$, the illumination distribution on the screen would become a straight line which means high uniformity. Based on this property, the uniformity could be improved.

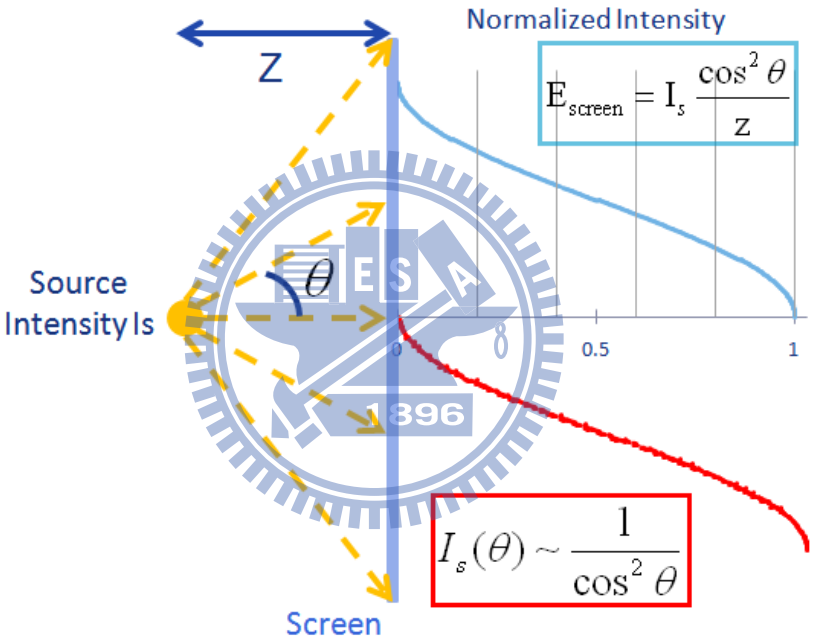


**Fig. 3.14** The blue line represented illuminance distribution via point source and the designed luminance intensity was red curve.

The discussion about the concept in Fig. 3.14 was an approximate process. Therefore, we could set 1-D linear light source in optical software to confirm this approximation was a correct method. According to the result in Fig. 3.15, the ideal and simulation curves were similar. It could believe that this reduction progress was usefully.

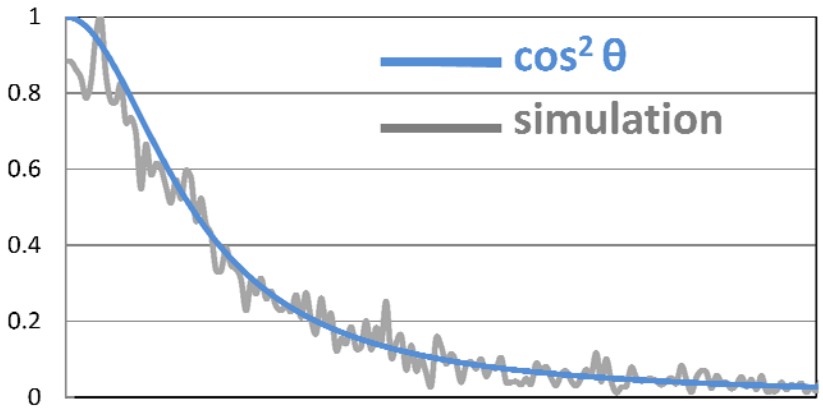


**Fig. 3.15** The gray line represented the simulation curve which could fit the $\cos^2\theta$ approximation

By this idea as motioned above, the light sources could be separated into three directions which as Fig. 3.16 to make the inverse cosine-square distribution introduced in the previous pages. Therefore, we could modify the opto-mechanism which was motioned in Fig. 3.6. In addition, a new opto-mechanism was proposed as Fig. 3.17 and the power ratio of each light bar could be adjusted to improve the uniformity.

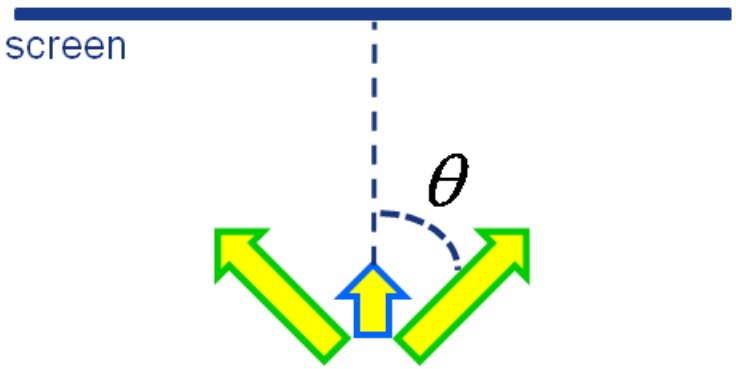


**Fig. 3.16** The light sources could be separated into three directions based on theoretic result to make the inverse cosine-square distribution, and then the hot spot issue could be fixed

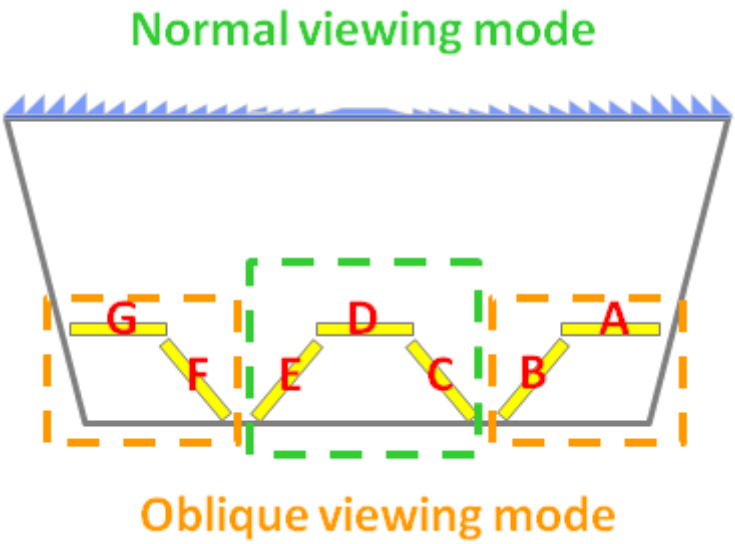


**Fig. 3.17** The new opto-mechanical structure of VAS backlight unit and the middle section (CDE) was used for normal viewing mode, and the other cluster (AB, and GF) were used for oblique viewing mode.

In brief, Fig. 3.17 shown the middle section was used for normal viewing mode as shown in the green dotted line. On the other hand, the other two clusters (AB and GF) were used for oblique viewing mode. Then, the inclined light bars (BCEF) were used to increase the luminance around the edge of the partition. In order to fit the $\cos^{-2}\theta$ optical field distribution, the power ratio of group (ADG) to group (BCEF) was 3, and the inclined angle of tilt plane with respect to the horizontal was 55°.

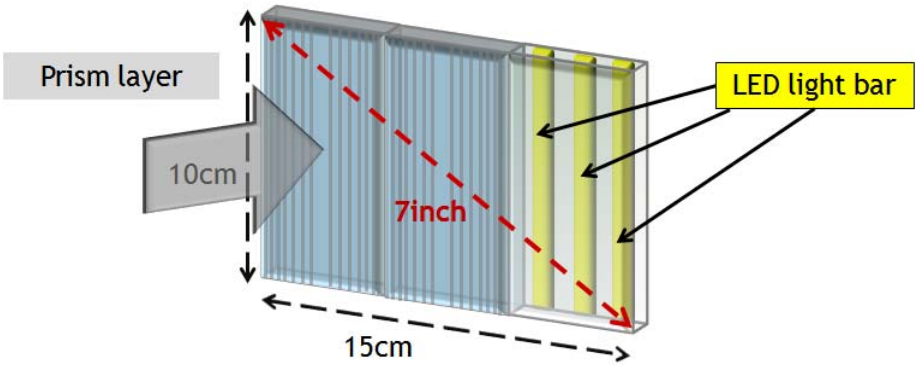


**Fig. 3.18** A 7 inch prototype was constructed by three sections of LED backlight units with the Fresnel lens

Since we are constrained by the fabrication issue, a 7 inch prototype was constructed by three LED backlight units with the Fresnel lens, as shown in Fig. 3.18. After confirming the final opto-mechanism, we could check the simulation result of uniformity improvement. The simulation outcomes were shown in Fig. 3.19 and Fig. 3.20. The uniformity of one unit was over 70%, which is better than our design target in Table 3.1. In addition, the FWHM of angular distribution is +/- 20 degree, which meet the requirements of design target [Table 2.1].

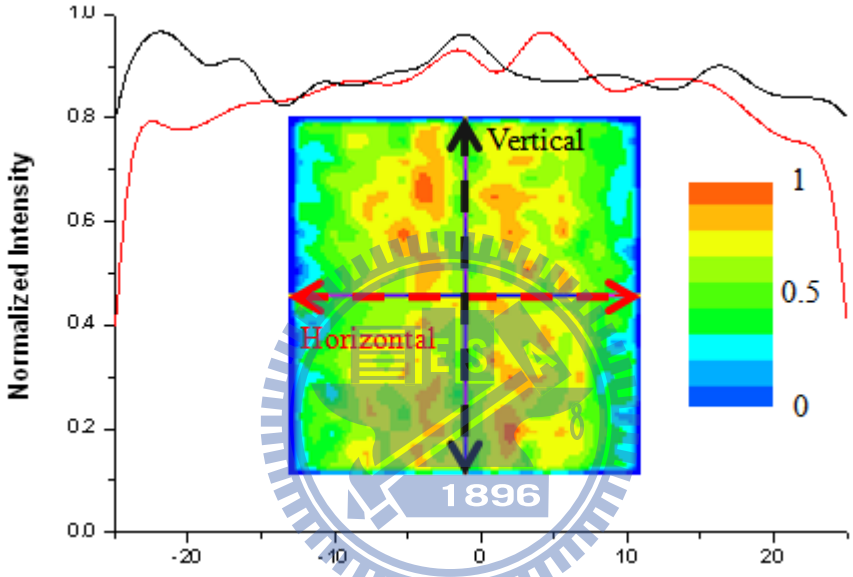


**Fig. 3.19** The simulation outcomes of normal mode uniformity

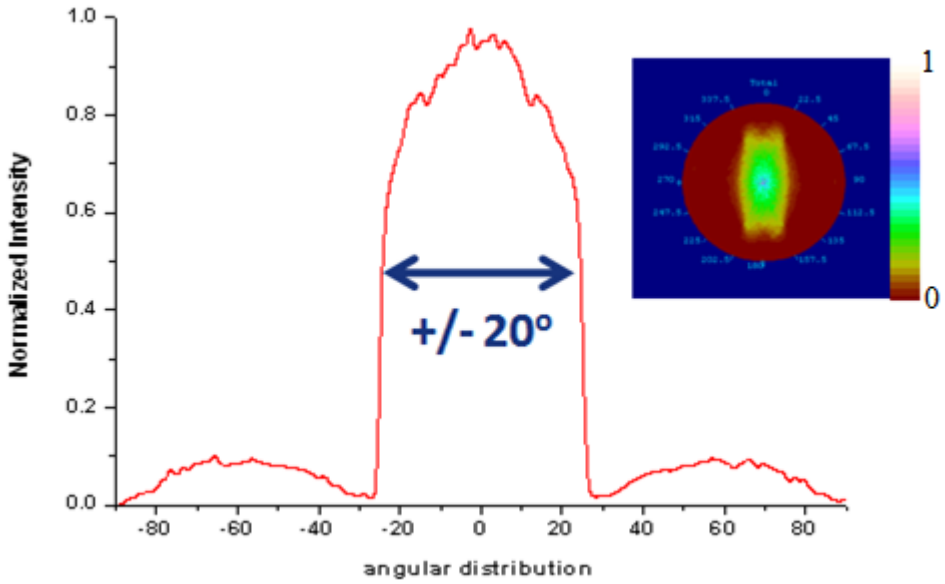


**Fig. 3.20** The simulation outcomes of angular distribution in normal mode

### 3.3 Simulation results for VAS backlight arrays

Fig. 3.21 represented the layouts of the VAS backlight units, turned on the middle and side parts of LED light bars were normal and oblique mode respectively. The uniformity of normal mode was over 80% that could fit in with the targets as shown in Fig.3.22. In addition, the FWHM of angular distribution of normal mode was confirmed between +/- 20 degree as Fig. 3.23 which could fit in with the design targets in Table 3.1.

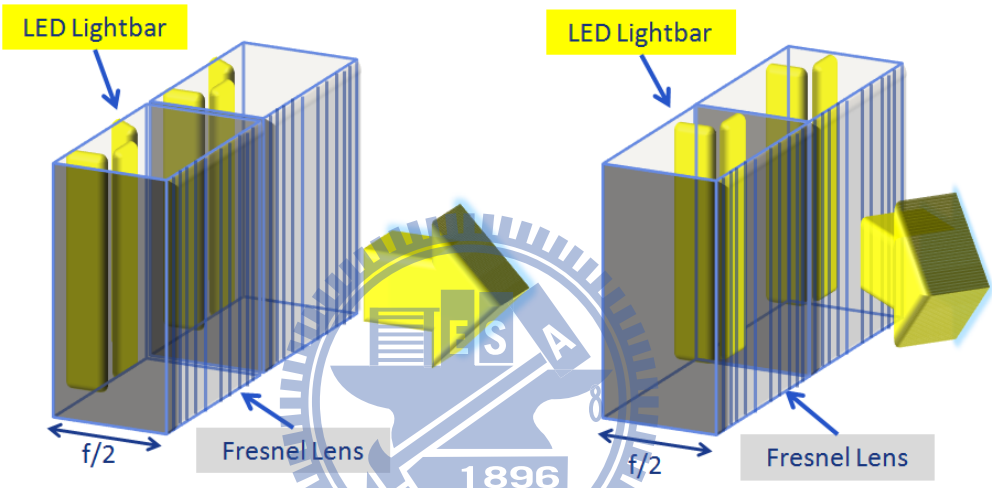


**Fig. 3.21** The simulation setups for (a) normal viewing mode and (b) oblique viewing mode in the optical simulation tool.

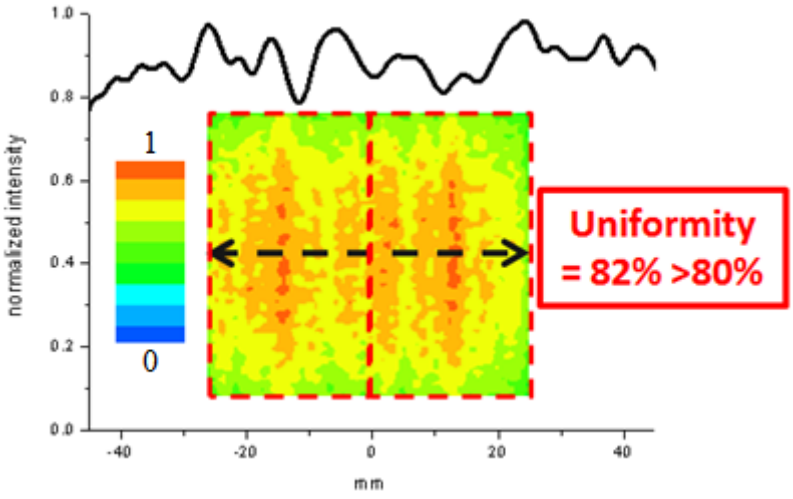


**Fig. 3.22** The simulation result of uniformity in normal viewing mode

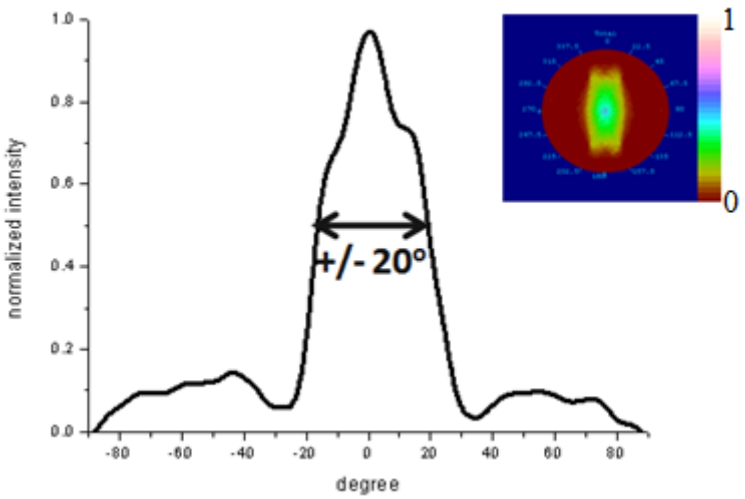


**Fig. 3.23** The angular distribution of normal viewing mode and the FWHM was +/-20°

However, the first compromise improved the uniformity of normal mode, but uniformity of oblique mode will not be good enough as shown in Fig. 3.24. If the power ratio was tuned for the uniformity of oblique mode again, it would decrease the location of peak value to 20 degree. Therefore, we had a trade-off between the uniformity and angular distribution of normal and oblique modes. If we wanted to increase the uniformity of oblique viewing mode, the viewing angle of oblique mode would be influenced. Therefore, a diffuser film will added into the entire opto-mechanism to solve the problem and then to improve the uniformity in oblique viewing mode.

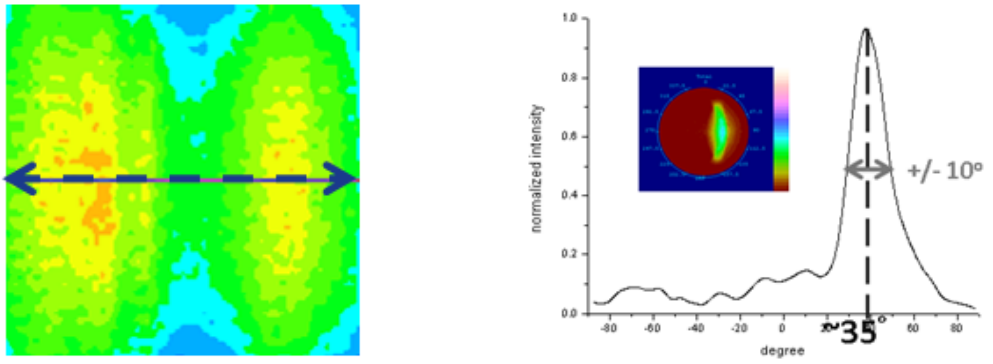


(a) (b)

**Fig. 3.24** The (a) uniformity and (b) angular distribution of oblique mode

# Chapter 4

# Experimental Results

## 4.1 Introduction

The concept of proposed viewing angle switchable backlight has been introduced in Chapter 3. Compared with the simulation, the experimental results of entire viewing angle switchable backlight module will be exhibited in this chapter.

The VAS backlight can be functioned as two kinds of modes (i.e. normal and oblique viewing modes). In normal viewing mode, the backlight offers a narrow optical field in the normal direction. On the other hand, the backlight offers an optical field in a fixed direction in oblique mode. The target of viewing angle control can be achieved by switching the LED light bars in our VAS backlight system.

## 4.2 Light Source Properties

The LED light bars were located at the bottom of the VAS backlight module, and each VAS backlight unit possessed seven light bars. One linear light bar contains 48 LED chips and phosphor layer as shown in Fig. 4.1. These two pictures showed the entire appearance of LED light bar, the placements of two electrodes, and the light

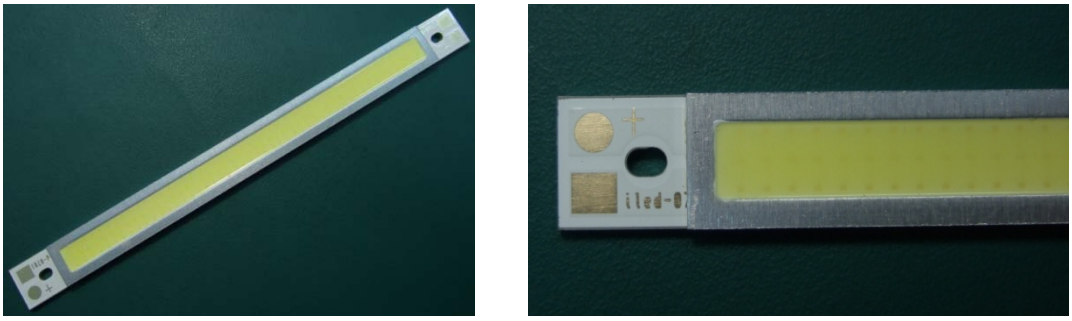

**Fig. 4.1** The white light LED light bar (iLED L03)

emitting region. In the experiment, the chromaticity of the LED light bar was (x, y) = (0.3035, 0.3199). In addition, the relative spectral distribution of the light bar was shown in Fig. 4.2. It is notable that the spectrum had two peaks in the ranges of blue and yellow wavebands which were induced by the LED chips and phosphor. The specification of the LED light bar was expressed in Table 4.1 in detail. The driving voltage can be adjusted according the table to control the actual luminance in our opto-mechanism and reach the inverse cosine square distribution [Chapter 3.2].

## 4.3 Light Control Prism Layer : Fresnel Lens

In the beginning of this thesis, a designed prism layer was proposed to redirect the light rays from the sources. Owing to the limit of some fabrication issues, the commercially available cylindrical Fresnel lens by Edmund Optics was adopted to replace the original prism layer. Hence, the following would be the detail information of this lens which is marshaled in Table 4.2. In addition, Fig 4.3 shows the cylindrical Fresnel lens by Edmund Optics. The red dash line in this picture represents the symmetric axis of this lenticular lens.

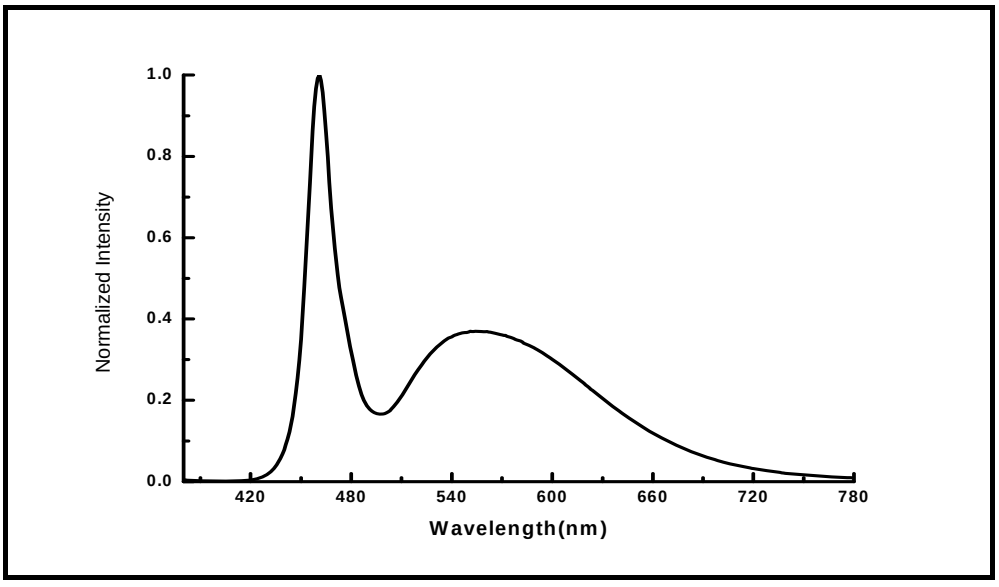


**Fig. 4.2** Spectrum distribution of white light LED light bar (iLED L03)

**[Table 4.1]** Electrical and optical characteristics of LED light bar (iLED L03)

| Parameter | Test Condition | Unit | MIN | TYP | MAX |
|---|---|---|---|---|---|
| Forward Voltage | $I_F$=240mA | V | 11.2 | 12.5 | 14 |
| Luminance | $I_F$=240mA | lm | 180 ~ 240 | | |
| Color Temperature | $I_F$=240mA | K | 5500 | 6300 | 6500 |
| Color-Rendering Index | $I_F$=240mA | | 70 ~ 80 | | |
| Viewing Angle | $I_F$=240mA | Degree | > 120 | | |

**[Table 4.2]** The specifications of Edmund Fresnel lens

| Size (inch) | F.L.* (inch) | Thickness (inch) | Refraction Index | T** | Grooves per inch |
|---|---|---|---|---|---|
| 2.0” x 12.0” | 2.0” | 0.06” | 1.49 | 92% | 200 |

* F.L. : Focal length, ** T : Transmission

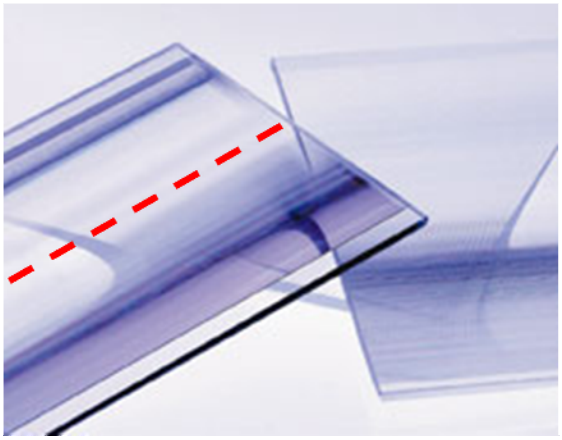

**Fig. 4.3** The Edmund cylindrical Fresnel lens

## 4.4 Experimental Setup

This paragraph showed the entire mechanism setup of the backlight module. As shown in Fig. 4.4, the VAS backlight unit included cylindrical Fresnel lens and seven LED light bars, and the locations of these light bards were coincident with Fig. 3.7. Furthermore, Fig. 4.5 exhibited the combined Fresnel lens. The original length of this lens was 12 inch as mentioned in Table 4.2. Therefore, the Fresnel lens was divided into three parts in practical mechanism. Eventually, 7 inch VAS backlight module could be fabricated with twenty one LED light bars and the combined Fresnel lens. Fig. 4.6 shows the upper Fresnel lens and the bottom LED light bars simultaneously, and Fig. 4.7 performs the actuated backlight module we've manufactured.

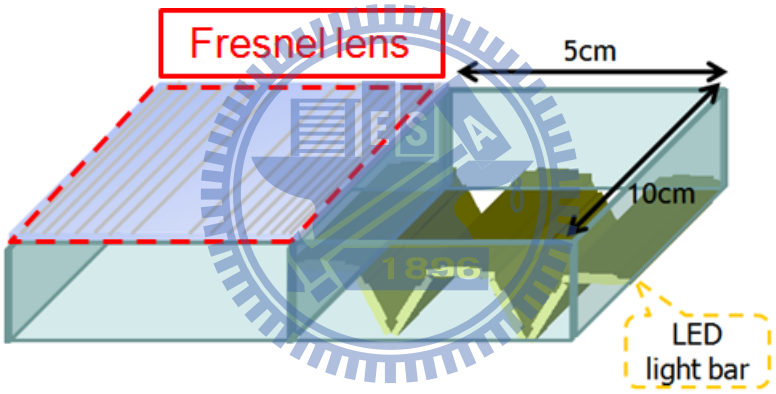


**Fig. 4.4** The Schematic configuration of entire mechanism setup for the actual VAS backlight module

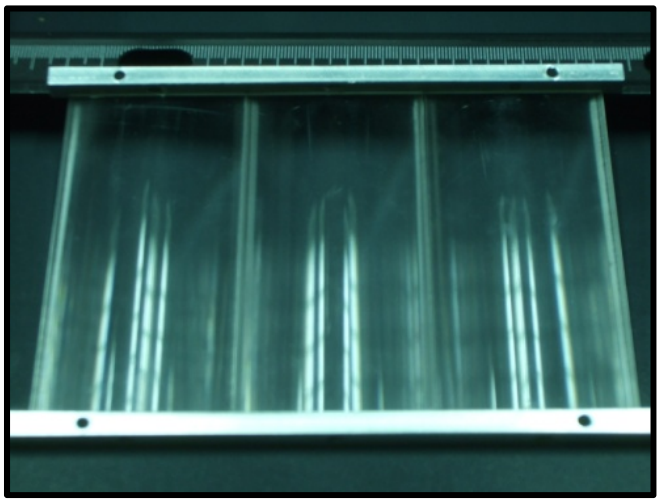

**Fig. 4.5** The combined Fresnel lens

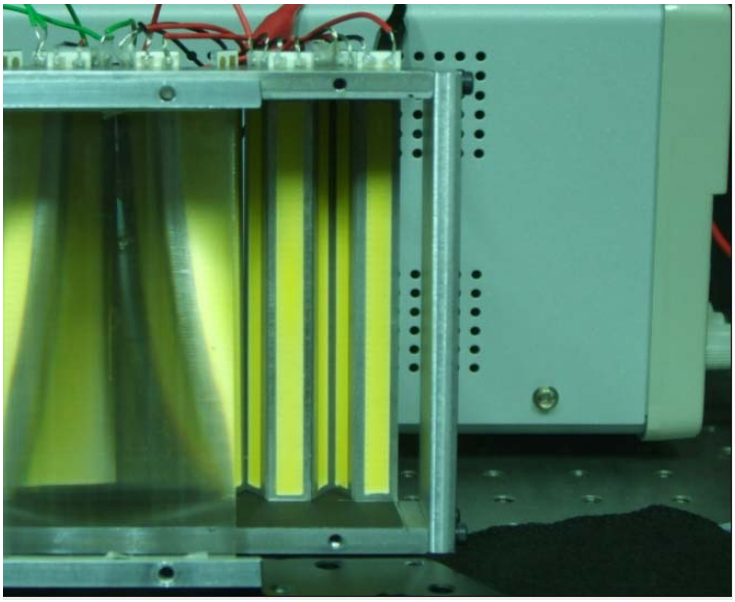

**Fig. 4.6** The apparatus was demonstrated which included the upper Fresnel lens and the bottom LED light bars

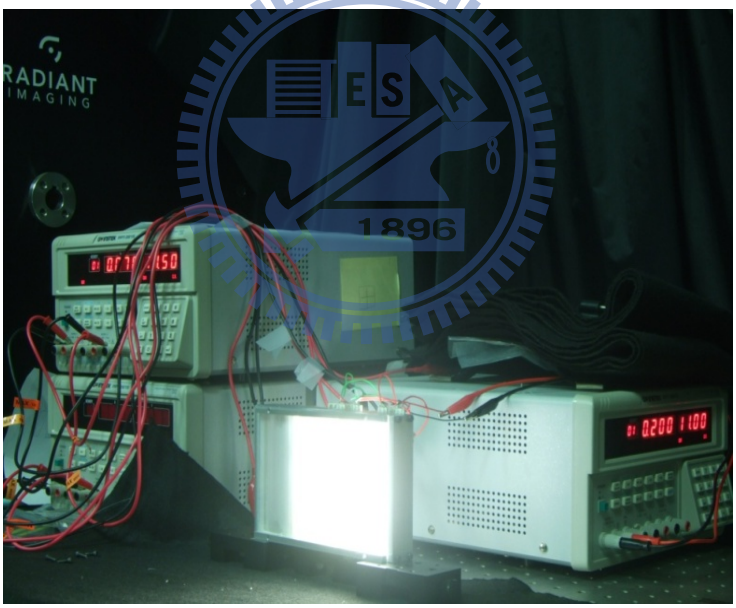


**Fig. 4.7** The entire VAS backlight module that we've manufactured was turned on

## 4.5 Measured Results : Normal and Oblique Viewing Modes

The results of cross-sectional luminance and angular distribution in one unit were exhibited for normal and oblique viewing modes in this section. As shown in Fig. 4.8 and Fig. 4.9, the green curves presented that the uniformity of normal and oblique

modes could reach 80% and 75%, respectively. In addition, the FWHM of angular distribution of these two modes were +/- 20 and +/- 15 degree as shown in Fig.4.8 and Fig. 4.9. All above data could reach the design target as introduced in chapter 3.1. Furthermore, the peak value of oblique mode in Fig. 4.9 (b) was located at 30 degree. The FWHM and the peak value of oblique mode were different from the simulation results. This diverse result should be induced by the stray lights via the inner surface of this backlight module.

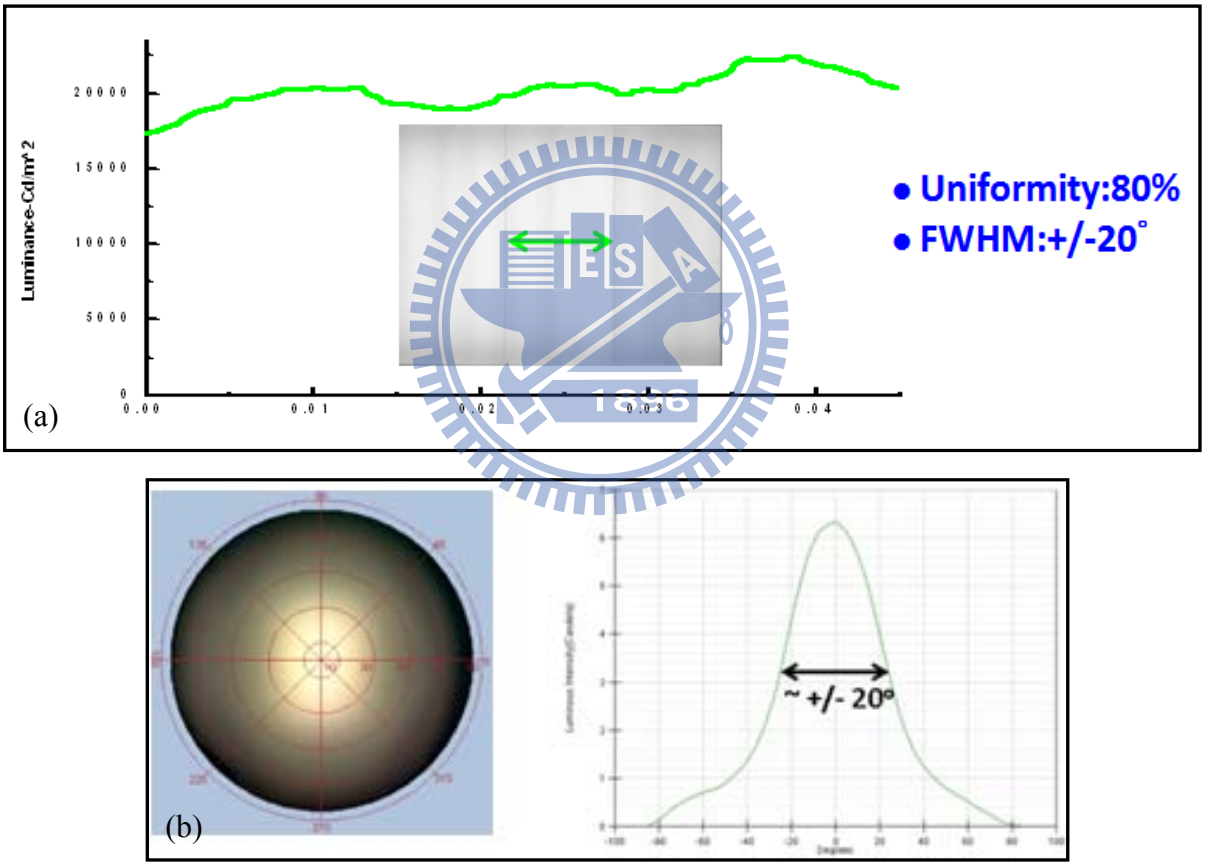


**Fig. 4.8** (a)The luminance map and the cross-sectional luminance curve with the uniformity of normal viewing modes was 80%; (b) The angular distribution of normal viewing mode with the FWHM +/- 20° by integral sphere.

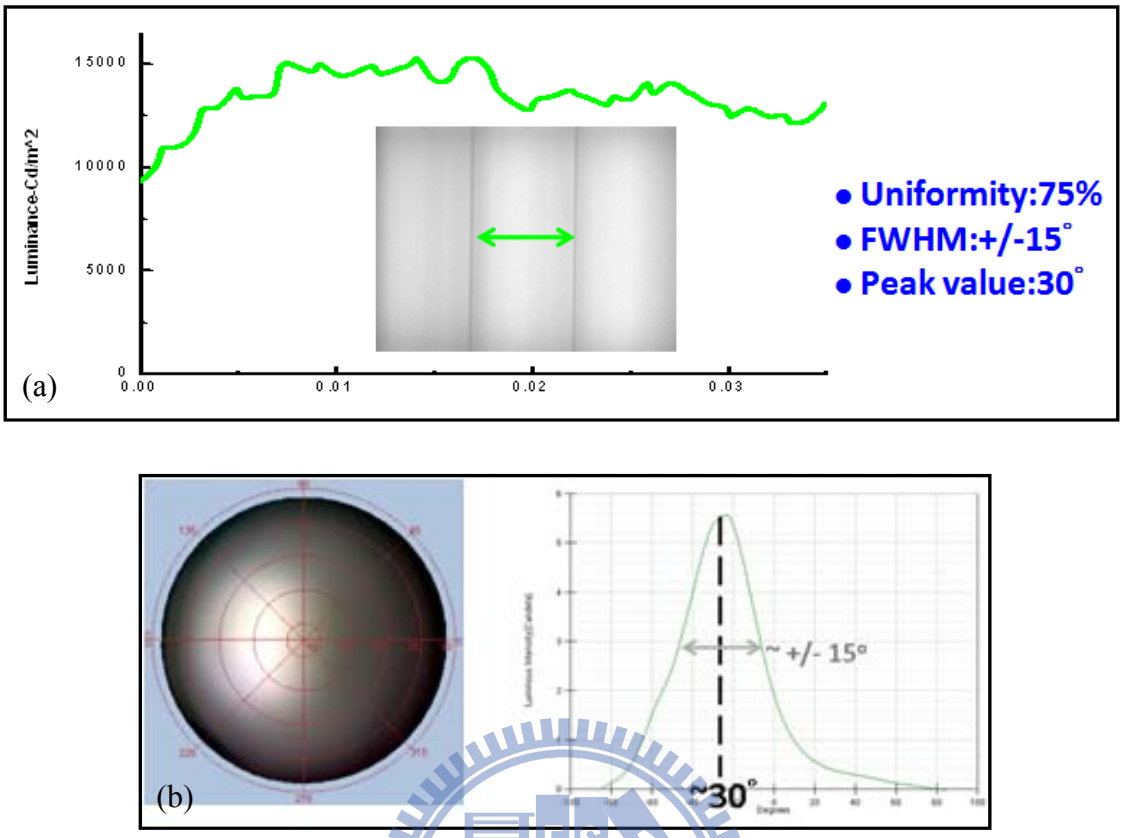


**Fig. 4.9** (a)The luminance map and the cross-sectional luminance curve with the uniformity of oblique viewing modes was 75%; (b) The angular distribution of oblique viewing mode with the FWHM +/- 20° by integral sphere.

# Chapter 5

# Conclusion and Future Work

## 5.1 Conclusion

In order to enhance the image quality and reduce power consumption in Eco-Display, the temporal, spatial, and angular modulation technologies of LED backlight shall play an important role in the future. Therefore, a prototype of the angular switchable backlight system with a 7-inch diagonal size had been accomplished and measured in this study. The developed module was shown in Fig. 4.7. Based on the novel opto-mechanical configuration shown in Fig. 3.17, the normal and oblique viewing mode can be switched by turning on the counterpart.

Table 5.1 exhibits the comparison of our VAS backlight module with the direct type backlight module. The targets of 70% uniformity and 0° to +/- 30° viewing angle control can be achieved. Besides, the most essential target, power consumption, would decrease to 30% and 50% in terms of normal and oblique modes, respectively. The optical performance of normal mode is realized with over 80% uniformity and angular distribution within +/- 20°. In addition, the luminance peaked sharply at 30° under oblique mode. Fig. 5.1 shows total performances of viewing-angle-switchable backlight. In the normal mode of BL, normal viewing has higher brightness than oblique viewing obviously. However, oblique viewing doesn't have obvious brightness difference under the BL oblique mode. Therefore, improving the BL uniformity in normal and oblique mode should be put on the top priority, and viewing angle control should be in the second place.

**[Table 5.1]** The comparison between direct and tunable type backlight module.

| BLM | Normal Mode | | | | Oblique Mode | | | |
|---|---|---|---|---|---|---|---|---|
| | U(%)* | L(nits)** | FWHM | P(watt) | U(%)* | L(nits)** | FWHM | P(watt) |
| Traditional Direct-type BLM | 80 | 23578 | ±35° | 11.4 | 80 | 22000 | | 11.4 |
| Our Angular Tunable BLM 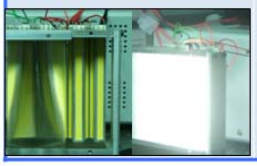 | 80 | 22587 | ±20° | 7.53 | 75 | 15596 | ±15° (@30°) | 5 |

*U: uniformity, ** L: Luminance

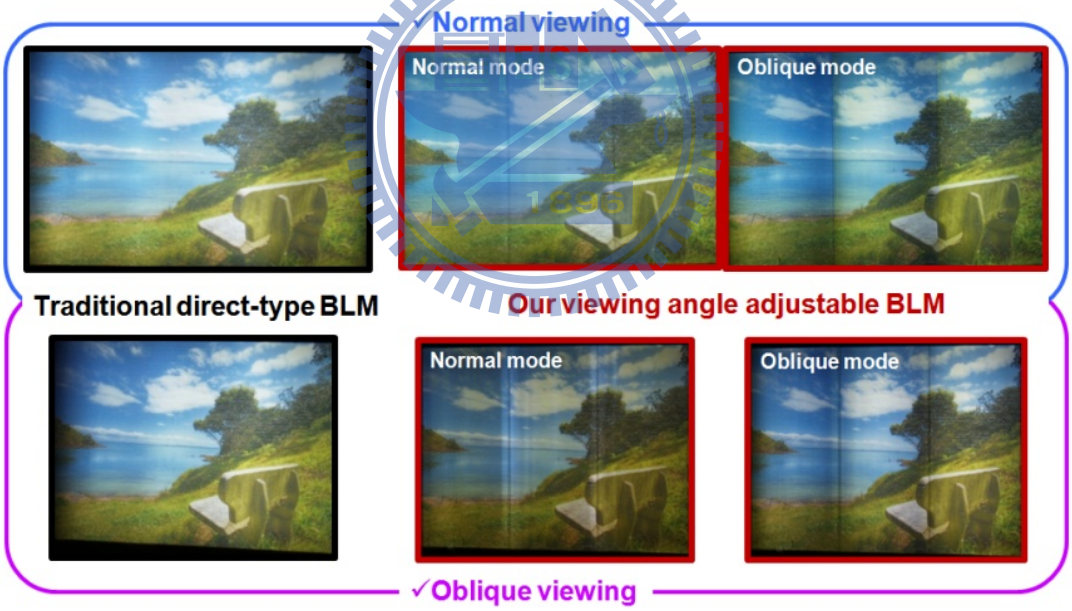


**Fig. 5.1** The performances of VAS backlight in normal and oblique mode for normal and oblique viewing conditions.

## 5.2 Future Work

In the future, the Fresnel lens shall be replaced by a designed prism layer to improve the performances in different operation states. According to Fig. 5.2, the

prism angle α corresponding to ray incidence ω can be precisely calculated. In addition, additional package for the LED light bar shall be modified to meet in our backlight requirement to decrease the stray light. The light flux from LED can be redistributed to meet the needs of lighting in the target plane by the secondary optical lens. This freeform lens is constructed by solving refractive equation and energy conservation numerically, and these numerical results can improve the illumination of uniformity near to 90%. For example, a designed LED package can perform uniform illumination on the target plane as Fig. 5.3 shows [15].

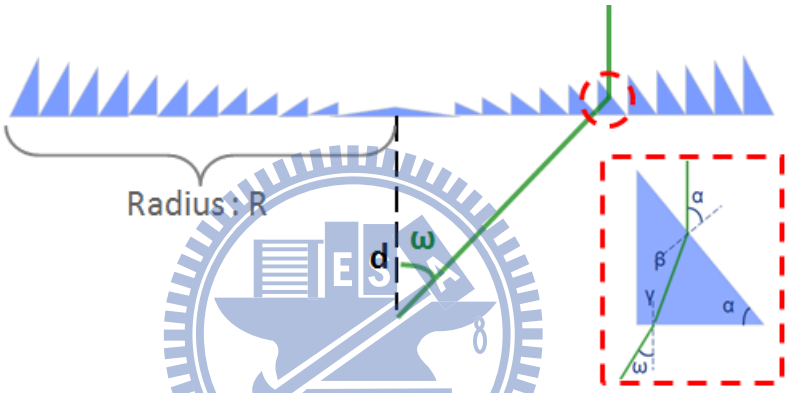


**Fig. 5.2** The Fresnel lens shall be replaced by a designed prism layer to enable the ray (i.e. green line) redirected for normal mode

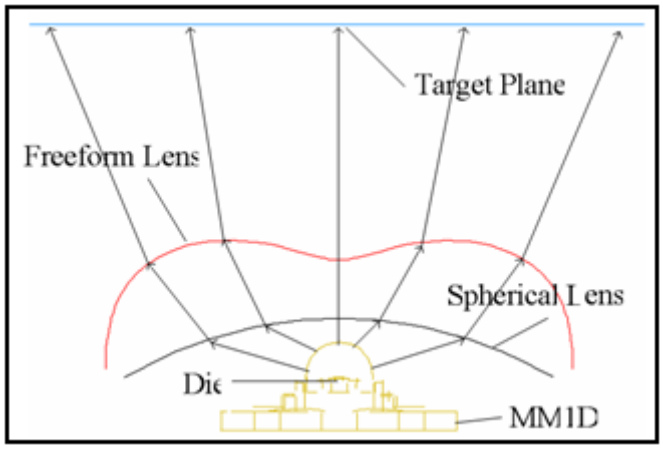


**Fig. 5.3** The designed package for LED light bar can meliorate the uniformity and stray light issue of the VAS backlight

# *Reference*


[1] M. Anandan, “Progress of LED backlights for LCDs,” *Journal of the SID 16/2*, pp. 287-310, (2008).

[2] Yoichi Taira, et al., “Color Filterless Liquid Crystal Display Illuminated with LEDs,” *SID International Symposium. Digest Tech Papers*, pp. 1250-1253,(2003).

[3] F. Yamada, et al., “Sequential-color LCD based on OCB with an LED backlight,” *Journal of the Society for Information Display*, Volume **10**, Issue **1**, pp. 81-85, 2004.

[4] Toni Jarvenpaa, “Measuring Color Breakup of Stationary Images in Field-Sequential-Color Displays,” *SID International Symposium. Digest Tech Papers*, 7.2, (2004).

[5] H. Seetzen, et al., “High Dynamic Range Display Systems,” *ACM Trans. on Graphics (Proc. of SIGGRAPH)*, **23(3)**: 760-768 (2004).

[6] E. Jeong, Y. J. Lim, J. M. Rhee, S. H. Lee, G.-D. Lee, K. H. Park, and H. C. Choi, “Viewing angle switching of vertical alignment liquid crystal displays by controlling birefringence of homogenously aligned liquid crystal layer,” *Appl. Phys. Lett*. **90,** 051116 (2007).

[7] J.-I. Baek, Y.-H. Kwon, J.C. Kim and T.-H. Yoon, “Dual-mode switching of a liquid crystal panel for viewing angle control,” *Appl. Phys. Lett.* **90,** 101104 (2007).

[8] S.-H. Oh and M.-H. Lee, “Liquid crystal display device having variable viewing angle,” US patent 7068336 (2006).

[9] Osamu Okumura , “Viewing angle control element, method of manufacturing the same, liquid crystal display device, and electronic apparatus,” US patent 7468770 (2008).

[10] K.-W. Chien, Y.-J. Hsu and H.-M. Chen, “Dual light source for backlight systems for smart viewing adjustable LCDs,” *Soc. Inf. Disp. Tech. Digest* **37**, 1425-1427 (2006).

[11] R. Leutz, A. Suzuki, “Nonimaging Fresnel lenses,” Springer, Berlin, p.35-39 (2001)

[12] A Davis, F Kuhnlenz, “Optical Design using Fresnel Lenses,” Optik & Photonik, p52-55 (2007)

[13] R. Leutz, A. Suzuki, “Nonimaging Fresnel lenses,” Springer, Berlin, p.67-68

(2001)

[14] R. Leutz, A. Suzuki, “Nonimaging Fresnel lenses,” Springer, Berlin, p.68-69 (2001)

[15] Yi Ding, Xu Liu, Zhen-rong Zheng, and Pei-fu Gu, "Freeform LED lens for uniform illumination," *Opt. Express* **16**, 12958-12966 (2008)